AFWL-TR-75-263

[redacted]WL-TR-
75-263
c./n-c

AD-A039657

ASYMPTOTIC CONICAL DIPOLE D-DOT SENSOR (ACD-S1(R)) DEVELOPMENT

Stewart L. Olsen

EG&G Inc.
9733 Coors Road, NM
Albuquerque, NM 87114

April 1976

Final Report

Approved for public release; distribution unlimited.

AIR FORCE WEAPONS LABORATORY
Air Force Systems Command
Kirtland Air Force Base, NM 87117

AFWL-TR-75-263

This final report was prepared by EG&G, Inc., Albuquerque, New Mexico, under Contract F29601-75-C-0085, Job Order 12090308 with the Air Force Weapons Laboratory, Kirtland Air Force Base, New Mexico. Captain Russell H. Bonn (ELS) was the Laboratory Project Officer-in-Charge.

This technical report has been reviewed and is approved for publication.

Russell H. Bonn

RUSSELL H. BONN
Captain, USAF
Project Officer

FOR THE COMMANDER

Thomas E. Morris

THOMAS E. MORRIS
Lt Colonel, USAF
Chief, Simulator Development
and Operations Branch

James L. Griggs Jr

JAMES L. GRIGGS, JR.
Colonel, USAF
Chief, Electronics Division

UNCLASSIFIED

SECURITY CLASSIFICATION OF THIS PAGE (When Data Entered)

REPORT DOCUMENTATION PAGE		READ INSTRUCTIONS BEFORE COMPLETING FORM
1. REPORT NUMBER AFWL-TR-75-263	2. GOVT ACCESSION NO.	3. RECIPIENT'S CATALOG NUMBER
4. TITLE (and Subtitle) ASYMPTOTIC CONICAL DIPOLE D-DOT SENSOR (ACD-S1(R)) DEVELOPMENT		5. TYPE OF REPORT & PERIOD COVERED Final Report 6. PERFORMING ORG. REPORT NUMBER
7. AUTHOR(s) Stewart L. Olsen		8. CONTRACT OR GRANT NUMBER(s) F29601-75-C-0085
9. PERFORMING ORGANIZATION NAME AND ADDRESS EG&G, Inc. 9733 Coors Road, NW Albuquerque, New Mexico 87114		10. PROGRAM ELEMENT, PROJECT, TASK AREA & WORK UNIT NUMBERS 64747F 12090308
11. CONTROLLING OFFICE NAME AND ADDRESS Air Force Weapons Laboratory (ELS) Kirtland Air Force Base, New Mexico 87117		12. REPORT DATE April 1976 13. NUMBER OF PAGES 42
14. MONITORING AGENCY NAME & ADDRESS(if different from Controlling Office)		15. SECURITY CLASS. (of this report) UNCLASSIFIED 15a. DECLASSIFICATION/DOWNGRADING SCHEDULE

16. DISTRIBUTION STATEMENT (of this Report)

Approved for public release; distribution unlimited.

17. DISTRIBUTION STATEMENT (of the abstract entered in Block 20, if different from Report)

18. SUPPLEMENTARY NOTES

19. KEY WORDS (Continue on reverse side if necessary and identify by block number)

Weapons Effects
Nuclear Explosions
Electromagnetic Sensors

20. ABSTRACT (Continue on reverse side if necessary and identify by block number)

This report describes the development of a small, D-dot sensor. The sensor shape is determined from the field distributions around a postulated line charge protruding from and normal to a conducting surface. It produces a voltage output in response to a time variant E-field. The theory of operation, modeling experiments, design and construction, prototype testing and test results are discussed within.

PREFACE

It should be recognized that Dr. Gary Sower, of EG&G, performed much of the preliminary design and assisted in specifying the final fabrication size and tolerance of the sensing element. My thanks is extended to Capt. Russell Bonn, of AFWL, who performed the pulse testing of the large prototype and assisted in the data reduction. Also special mention is due Mr. Jon Melville and his sensor lab staff who performed their usual diligent and exacting work in building this extremely small sensor.

CONTENTS

LIST OF ILLUSTRATIONS

SECTION I
INTRODUCTION

The ACD-S1A(R) D-dot sensor (Asymptotic Conical Dipole - see Figure 1) was developed under AFWL Contract No. F29601-75-R-0085. The objective was to complement the existing line of D-dot sensors with another standardized laboratory sensor having small physical dimensions and corresponding high frequency response, to facilitate EMP testing of scale model objects. This effort resulted in the development of a scaled-up (10:1) prototype for equivalent area and frequency response verification, a to-scale prototype to assess the fabrication problems at the extremely small size, and three production sensors.

The ACD-S1A(R), having an equivalent area of 10^{-4} square meter, has a sensing element which is coincident with an equipotential surface from a postulated line charge of known height and dipole moment. It is mounted on a ground plane and has an OSSM output connector. The upper frequency 3 dB point is estimated at over 7.5 GHz. The sensor is designed for use in a laboratory environment and has no weather cover. A dielectric dome is provided for mechanical support and protection. This sensor was also produced in a version with a flexible section of ground plane between the sensing element and the output connector. It is designated as ACD-S1B(R) and has identical characteristics.

This effort was paralleled by the design and construction of a B-dot sensor, having similar design goals for scale model testing.[1]

[1]Olsen, Stewart, MGL-S8 B-Dot Sensor Development, 10 September 1975, EG&G Report No. AL-1187, AFWL-TR-75-252.

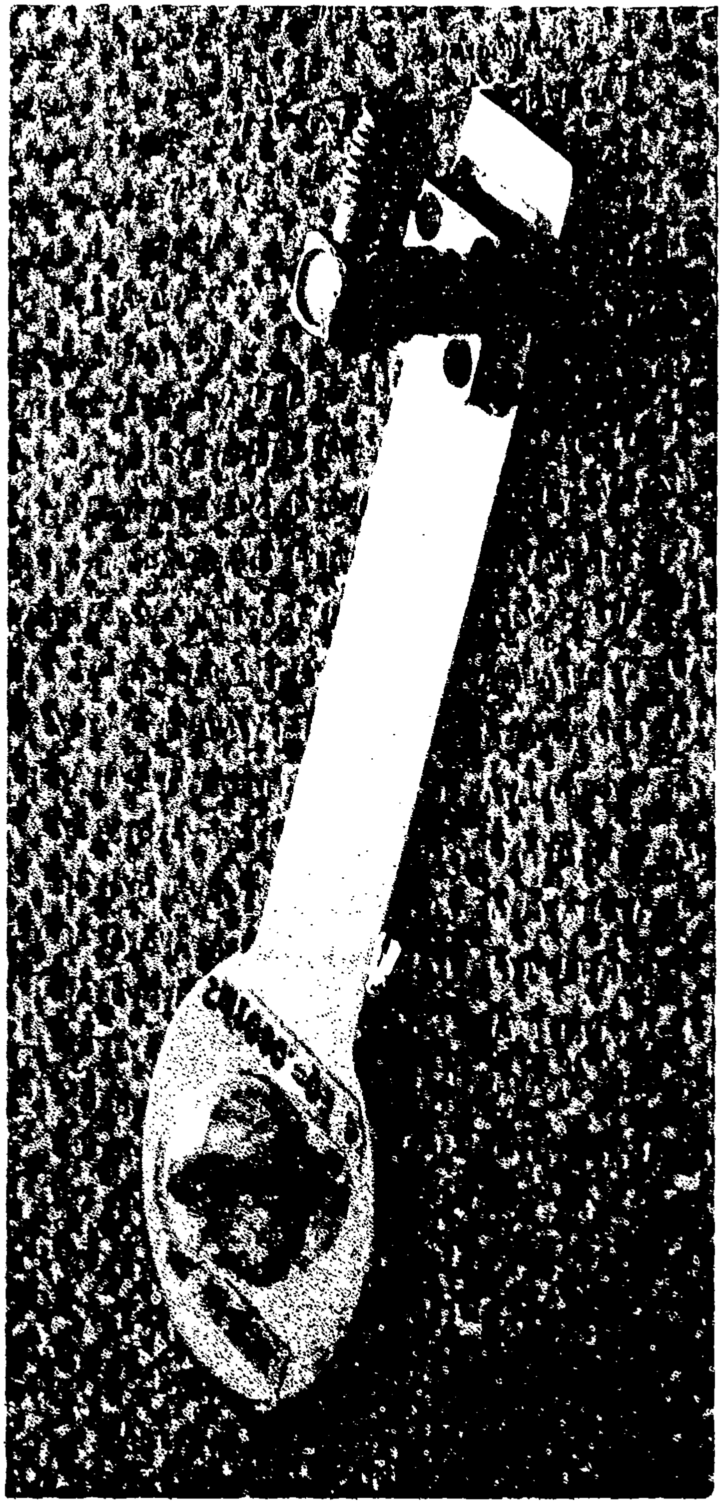

Figure 1. ACD-S1A(R) D-Dot Sensor

SECTION II
THEORY OF OPERATION

1. BASIC SENSOR TRANSFER FUNCTION

The transfer function of an asymptotic conical dipole D-dot sensor is readily derived by application of the integral form of Gauss's Law to the situation depicted in Figure 2: an asymptotic conical conducting surface positioned over a ground plane as shown, with a D-field directed normal to the ground plane. Gauss's Law states that:

$$\int \vec{D} \cdot d\vec{A} = \int \rho dv \qquad (1)$$

where dA is a differential element of area on a Gaussian surface which just encloses the conductor, dv is a differential element of the volume enclosed by the surface, and ρ is the charge density. Integrating equation (1) yields:

$$A'D = \rho v = Q \qquad (2)$$

where A' is a constant having units of area, v is the total volume contained within the surface and Q is the total charge on the conducting surface. The coefficient of D in equation (2), A', determines the sensitivity of the sensor and is defined as the equivalent area, A_{eq}, of the asymptotic conical conductor. Using this definition, we can rewrite equation (2) as:

$$A_{eq} D = Q \qquad (3)$$

The equivalent area can be calculated from reference 2 and is given in Appendix A. Differentiating equation (3) with respect to time,

$$\frac{d}{dt} A_{eq} D = \frac{dQ}{dt}$$

[2] Baum, Carl E., An Equivalent-Charge Method for Defining Geometries of Dipole Antennas, 24 January 1969, AFWL SSN 72.

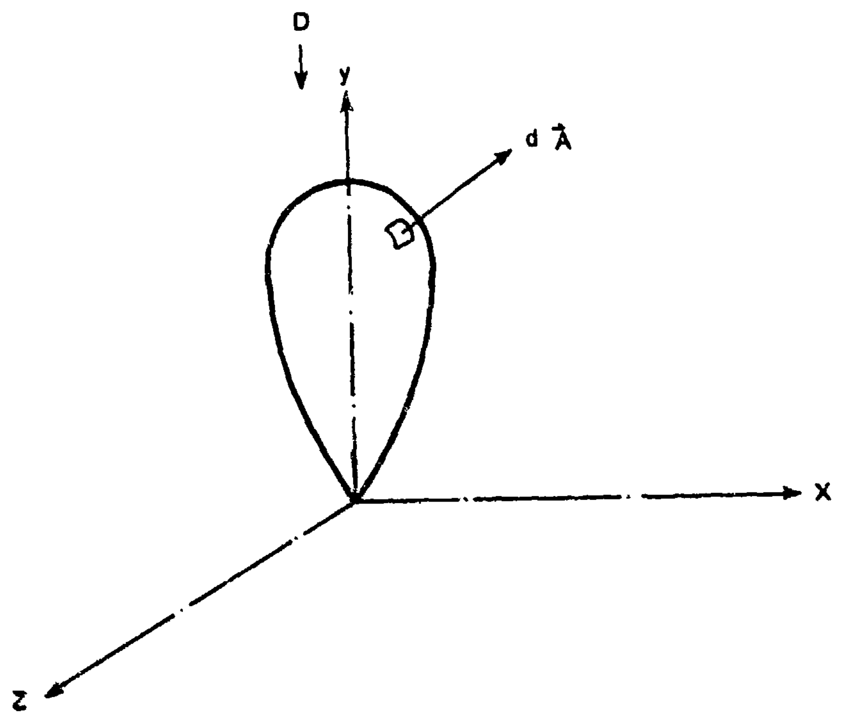

Figure 2. Asymptotic **Conical Conductor Above a Ground Plane**

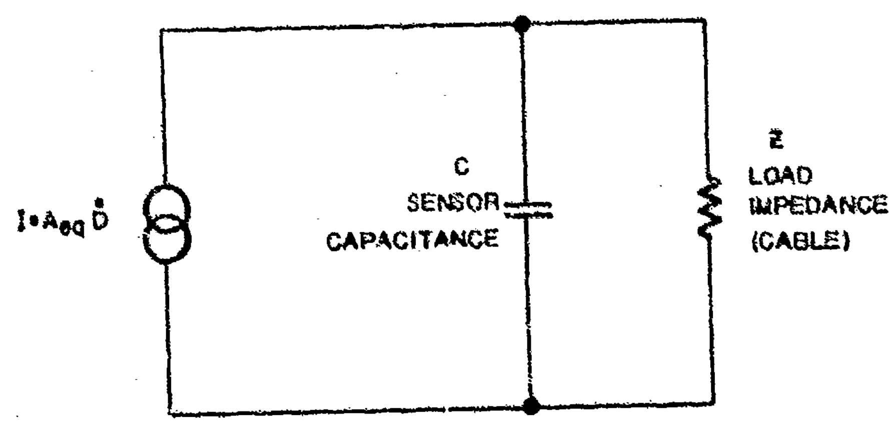

Figure 3. Equivalent Circuit of D-dot Sensor

or,

$$A_{eq}\dot{D} = I = C\frac{dV}{dt} + \frac{V}{R} = C\dot{V} + \frac{V}{R} \qquad (4)$$

where I is the current flowing from the sensing element to the ground plane through the equivalent circuit shown in Figure 3, C is the capacitance between the sensing element and the ground plane, V is the voltage across the load and R is the impedance of the load, which in the case of a sensor is the impedance of the output cable. Equation (4) may be solved for V by means of Laplace transformation to the frequency domain. The Laplace transform of equation (4) is:

$$A_{eq}sD(s) = CsV(s) + \frac{V(s)}{R}$$

where $s = j\omega$.

Solving for V(s)

$$V(s) = \frac{A_{eq}sD(s)R}{RCs + 1} \qquad (5)$$

2. FREQUENCY RESPONSE

The transfer function as shown in equation (5) is not very convenient in actual practice: fortunately, we can often simplify the transfer function to a low or high frequency approximation. At low frequencies (Frequencies below 0.75 GHz), RCs (= $RCj\omega$) is small compared to 1 and therefore can be neglected. The transfer function then becomes:

$$V(s) = A_{eq}sD(s)R$$

Transforming back to the time domain,

$$V = A_{eq}\dot{D}R \qquad (6)$$

is the low frequency transfer function.

At higher frequencies (above 75 GHz), RCs is large compared to 1 and the transfer function then becomes:

$$V(s) = \frac{A_{eq} sD(s)R}{RCs} = \frac{A_{eq} D(s)}{C}$$

transforming back to the time domain,

$$V = \frac{A_{eq} D}{C} \tag{7}$$

the high frequency transfer function.

When RCs = 1, it can be shown that the error in either equation (6) or (7) is =3 dB. This frequency (7.5 GHz) thus defined is the transition frequency. The relationship between the three transfer functions is shown in Figure 4. The transition frequency is calculated by substituting the absolute value of s in the defining relation:

$$RC\,|s| = RC\,|j\omega| = RC\omega_t = 1$$

$$\omega_t = \frac{1}{RC}$$

$$f_t = \frac{1}{2\pi RC} \tag{8}$$

The transition frequency is shown later in this report to be 7.5 GHz. The .3 dB error values are then 750 MHz and 75 GHz, also shown in Figure 4.

3. SURFACE CHARGE DENSITY TRANSFER FUNCTION

From equation (3), we see that the imposed electric field draws a charge to the surface of the ground plane. The D-dot sensor also measures the D-field generated when a charge is placed on the ground plane, thus,

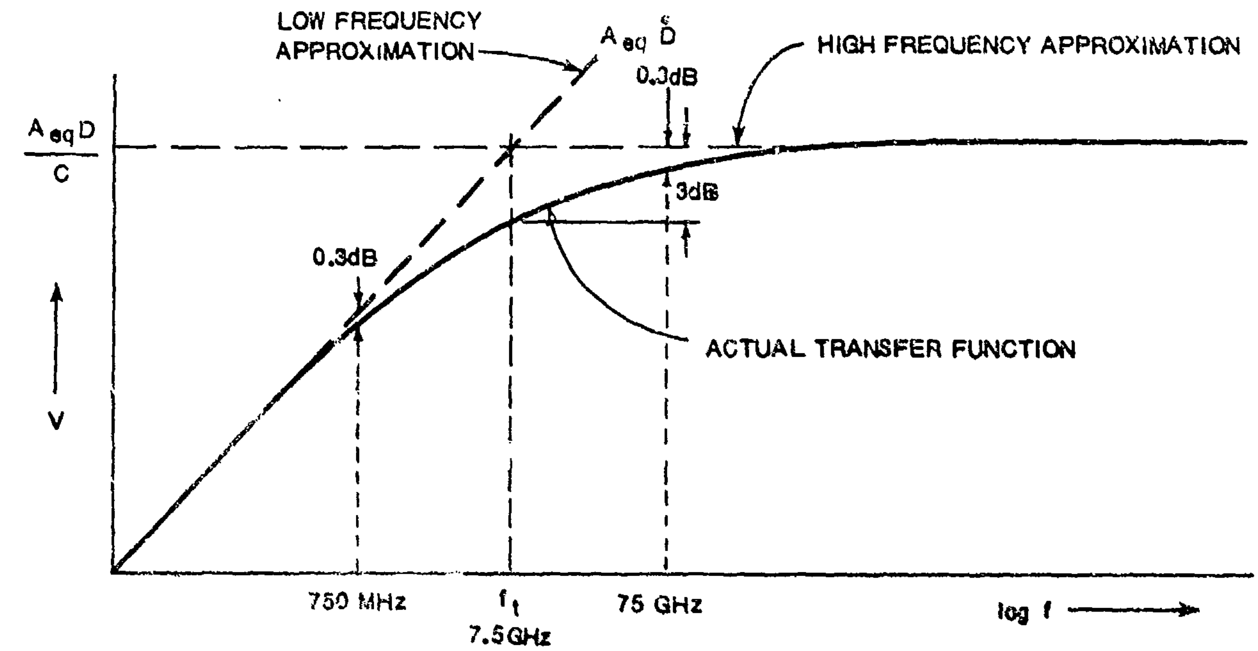

Figure 4. Frequency Response of D-dot Sensor

rewriting equation (3):

$$\dot{D} = \frac{\dot{Q}}{A_{eq}}$$

and the sensor output becomes:

$$V_{out} = \dot{D}\ A_{eq}R = \dot{Q}R \tag{9}$$

and is subject to the same frequency domain treatment of paragraph 1.

SECTION III
LARGE PROTOTYPE

Because of the small size of the ACD-S1A(R) ($1 \times 10^{-4} m^2$), the verification of its equivalent area as well as its frequency response was performed on a scaled-up model that was ten times larger in dimension than the actual ACD-S1A(R). This represents an equivalent area of $1 \times 10^{-2} m^2$ for the large prototype.

1. OVERALL CONFIGURATION

The ACD-S1A(R) D-dot sensor large prototype is shown in Figure 5. The sensing element is connected, at the base, to a 50 ohm semi-rigid cable which then passes within the ground plane to an OSSM connector. The sensing element is then covered with a thin, dielectric shell which protects and supports the element.

2. DIMENSION CALCULATIONS

The surface of the ACD-S1A(R) sensor, as derived by C.E. Baum[2], was to be on a contour of constant potential generated by a line charge protruding from, and normal to, the ground plane. The details are found in Appendix A, along with the computer program for generating the contour for a desired A_{eq}. Because of great difficulty and expense involved in accurately determining the area perturbation due to the base plate, the dome, support washer, etc., it was directed by the AFWL that the equivalent area be made 2% low as an estimate of compensation. The final height selected was 2.229 inches for the large prototype.

The base plate dimensions were determined by:

- requiring the connector be at least ten sensor heights from the sensing element,
- requiring that the ground plate be thick enough to support the sensor and connector while containing the output cable,
- requiring that the edge of the base plate was at least two sensor heights from the sensing element.

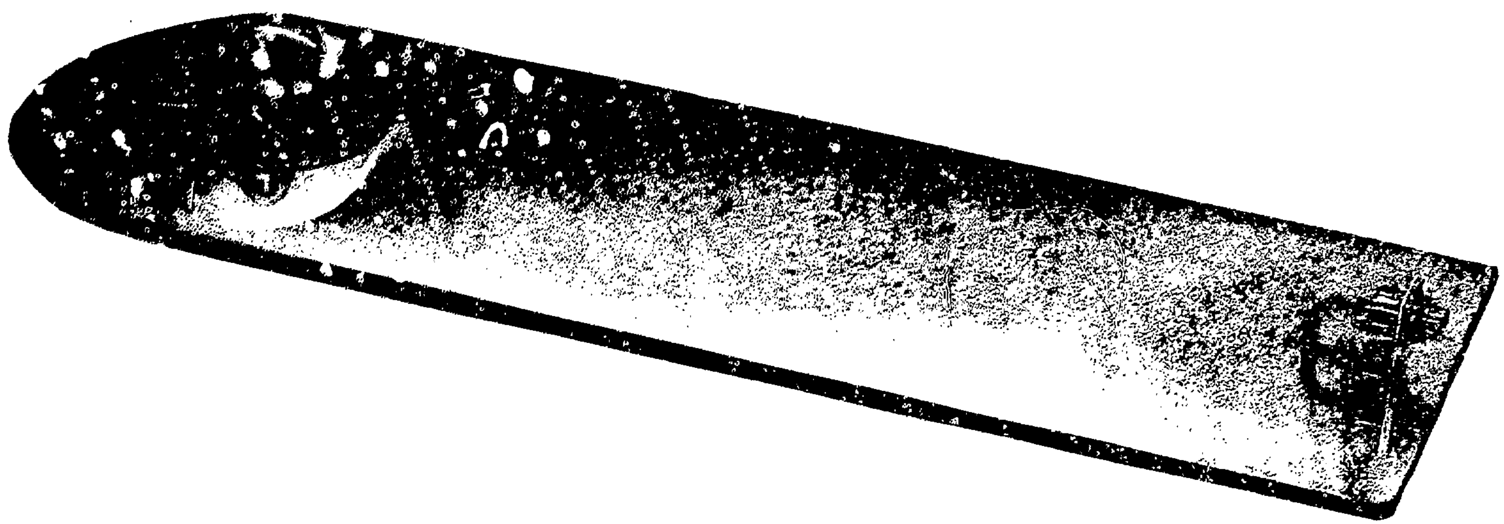

Figure 5. ACD-S1A Large Prototype D-Dot Sensor

These requirements were chosen to minimize the baseplate perturbation of the electric field near the sensing element. The resulting baseplate dimensions are a 0.400 inch thick aluminum plate 30 inches long by 10 inches wide as shown in Figure 5.

3. PROTECTIVE DOME

To support the sensing element above the ground plane while protecting it from damage, a shell was built to cover the sensing element. Several methods had been considered including a dielectric grid and a foamed dielectric encapsulant.

Another method considered was an epoxy encapsulant. This would be advantageous and practical for a very small sensing element in a large epoxy hemisphere, but when the sensor size becomes large compared with the solid dome, the fields and the sensor area are not readily calculable.

The dome used is a (lucite) hemisphere which has a hole in the top for bonding to the top of the sensing element. The dome is mounted in a registration slot around the sensing element, keeping the sensor vertical. For lucite, ϵ_r is 2.5. This will cause a slight enhancement in the sensor equivalent area. The shell is very thin-walled (2.54×10^{-4}m) to minimize this effect. During sensor testing the dome was removed and about 1.3% change in A_{eq} noted.

4. UPPER FREQUENCY LIMIT

The frequency where the sensor output is 3 dB below its ideal response is directly related to the capacitance between the sensing element and the ground plane and to the transit time associated with its physical dimensions. The capacitance, obtained from the analysis of Appendix A, is 1.7 pF. For a RC risetime defined by

$$T_{r_c} = 2.2\,RC \tag{10}$$

we have a risetime of 0.187 ns for a 50 ohm cable load at the apex of the sensor.

The transit time limitation results from the round-trip time along the surface of the sensing element. An analogy can be drawn to the results

of SSN 8[3], where a loop is shown to be equivalent to a parallel wire transmission line (of length π a) terminated in a short circuit (illustrated in Figure 6a). Here we have a parallel transmission line terminated in an open circuit. The length of the line being roughly the distance, along the surface from the apex to the top of the sensing element (Figure 6b). For a sensing element of 2.29 inches in height, the distance ℓ_s is 2.62 inches. Again, borrowing from SSN 8 we can take the equivalent risetime approximation to be

$$T_{r_t} = \frac{2\ (\ell)}{c} = 0.44 \text{ ns} \tag{11}$$

where ℓ is the transit distance (2.62 inch = .0665 m), c = velocity of light. Adding the transit limitation and the RC limitation in quadrature we get

$$T_r = 0.48 \text{ ns}$$

for the risetime of the ACD large prototype corresponding to a bandwidth (using the T_r x BW = 0.35 definition) of 727 MHz.

5. LARGE PROTOTYPE - TESTING

Pulse testing and data evaluation were performed by the AFWL at the conical simulator facility at Kirtland Air Force Base.

a. Pulse Response

The response of an ideal differentiating sensor to a step function input (shown in Figure 7a) is a delta function of infinite height and zero width.

Figure 7b indicates the response an ideal sensor would produce for a typical (Gaussian) pulse with finite risetime, T_r. If this response is integrated and the 10 to 90% risetime (T_r) of the resulting step function measured, it will be nearly equal to the time between the half amplitude points of the Gaussian pulse.

[3] Baum, Carl E., Maximizing Frequency Response of a B-Dot Loop, 9 December 1964, AFWL SSN 8.

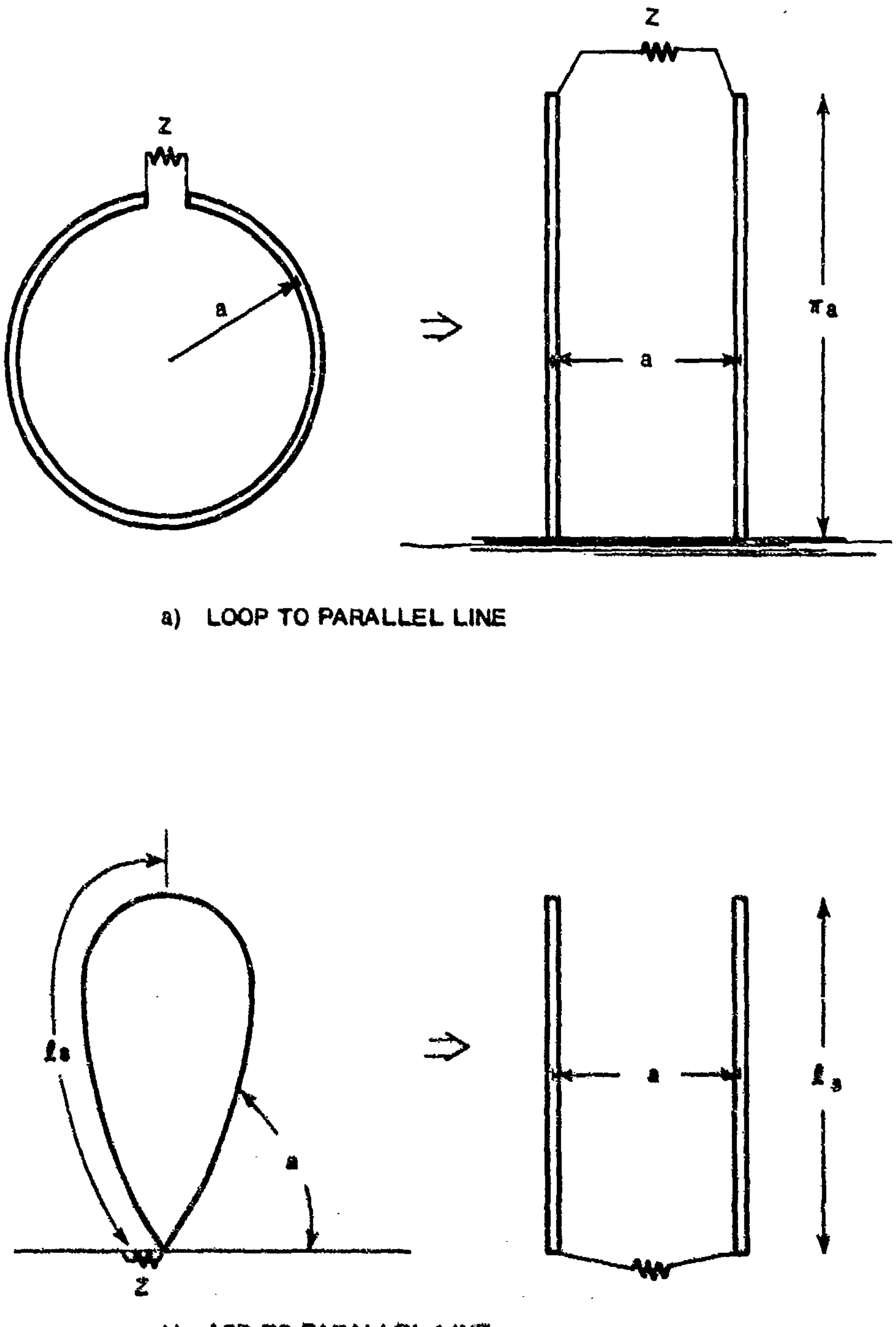

Figure 6. Appropriate Transformations to Observe Effective Length

A distortion occurs if a real sensor with finite risetime (limited frequency response) could be exposed to a perfect step function as illustrated in Figure 7c. Again, the measured risetime of the integrated output response is very nearly equal to the half width points of sensor output and is the risetime of the sensor T_{r_2}.

A real case, of course, involves an incident field of finite risetime and a sensor with a limited frequency response. As one might suspect, the recorded output and integrated output show a risetime greater than either T_{r_1} or T_{r_2}. This is illustrated in Figure 7d. The square of the measured risetime is taken to be (for Gaussian curves) equal to the sum of the squares of the incident field and sensor risetimes and will be used to obtain the sensor risetime. The equivalent area can be verified by comparing the integral of the sensor output to the amplitude of the applied field. The transfer function is

$$Z A_{eq} \dot{D} = V_o \qquad (12)$$

where Z is the output cable impedance. Integrating both sides with respect to time

$$Z A_{eq} D = \int V_o(t)dt$$

or

$$A_{eq} = \frac{\int V_o(t)dt}{ZD} \qquad (13)$$

The pulse response tests were done with the test setup shown in Figure 8. A description of the test setup follows.

- The conical test fixture is a 15-foot high by 3-foot maximum diameter copper screen cone with a conic angle $\theta = 5.712$ and its apex at the center of a 30 foot diameter copper screen ground plane. Figure 9 shows a photograph of this simulator. This structure forms a conical transmission line of 180 ohms.[4]

[4]Baum, Carl E., A Circular Conical Antenna Simulator, 3 March 1967, AFWL SSN 36.

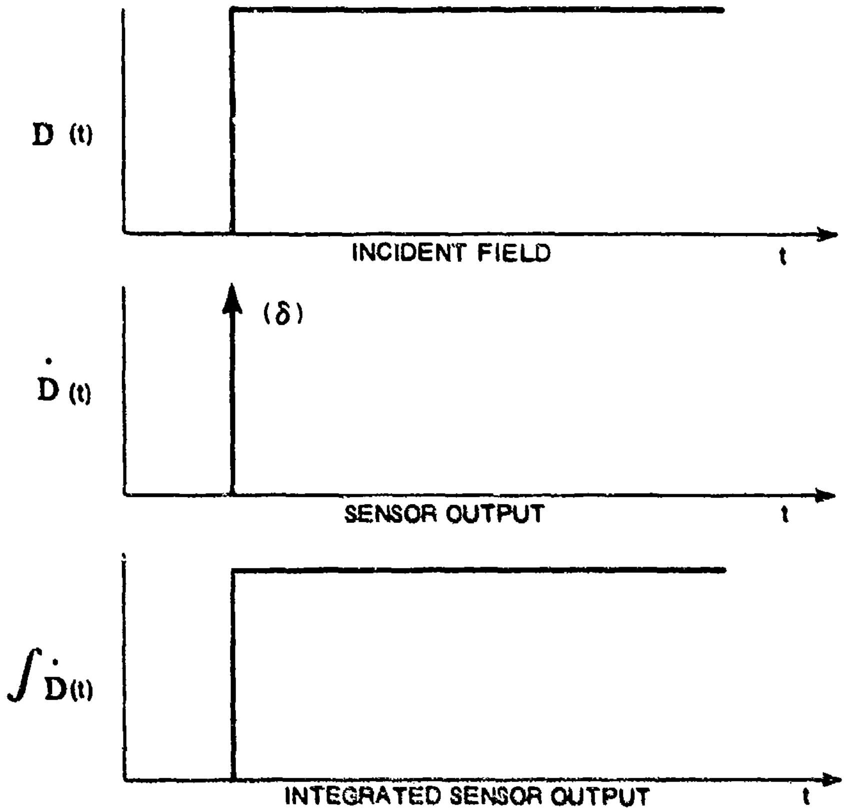

Figure 7a. Ideal Sensor and Ideal Pulse

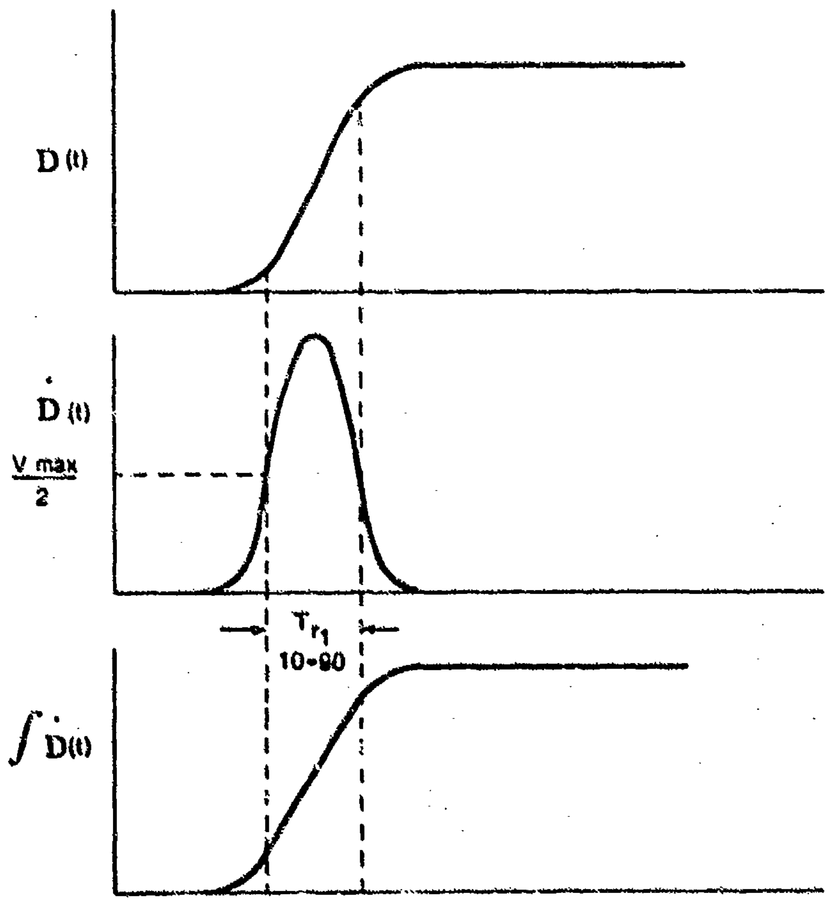

Figure 7b. Ideal Sensor and Nonideal Pulse

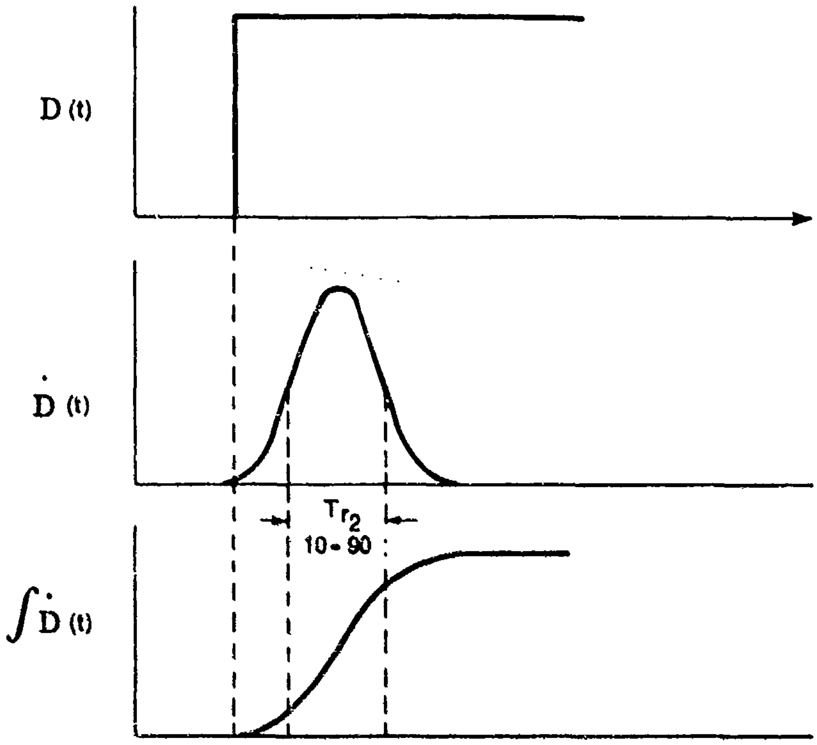

Figure 7c. Nonideal Sensor and Ideal Pulse

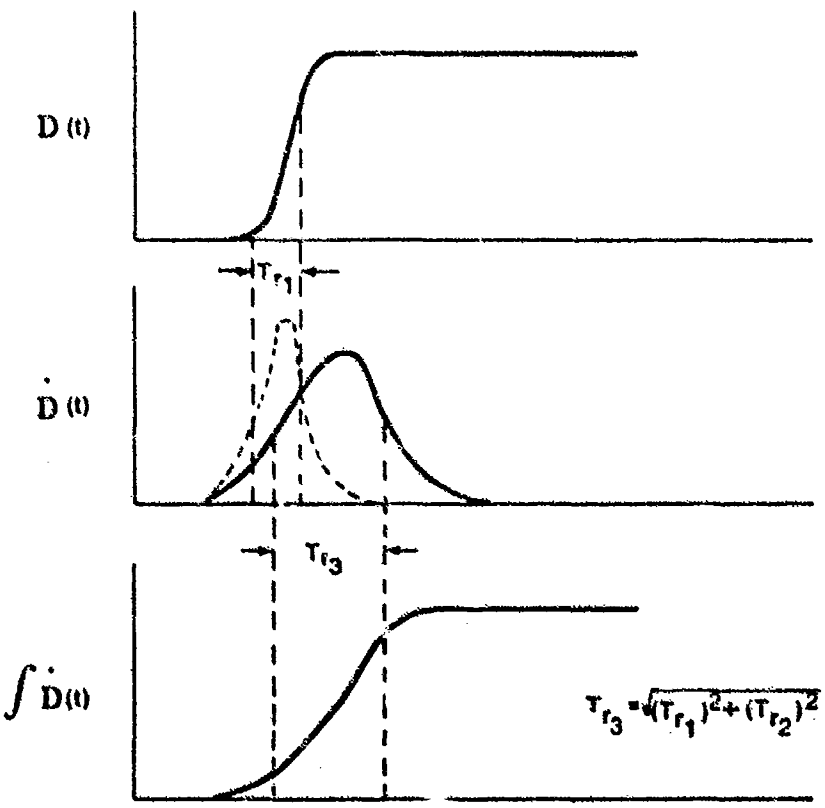

Figure 7d. Nonideal Sensor and Nonideal Pulse

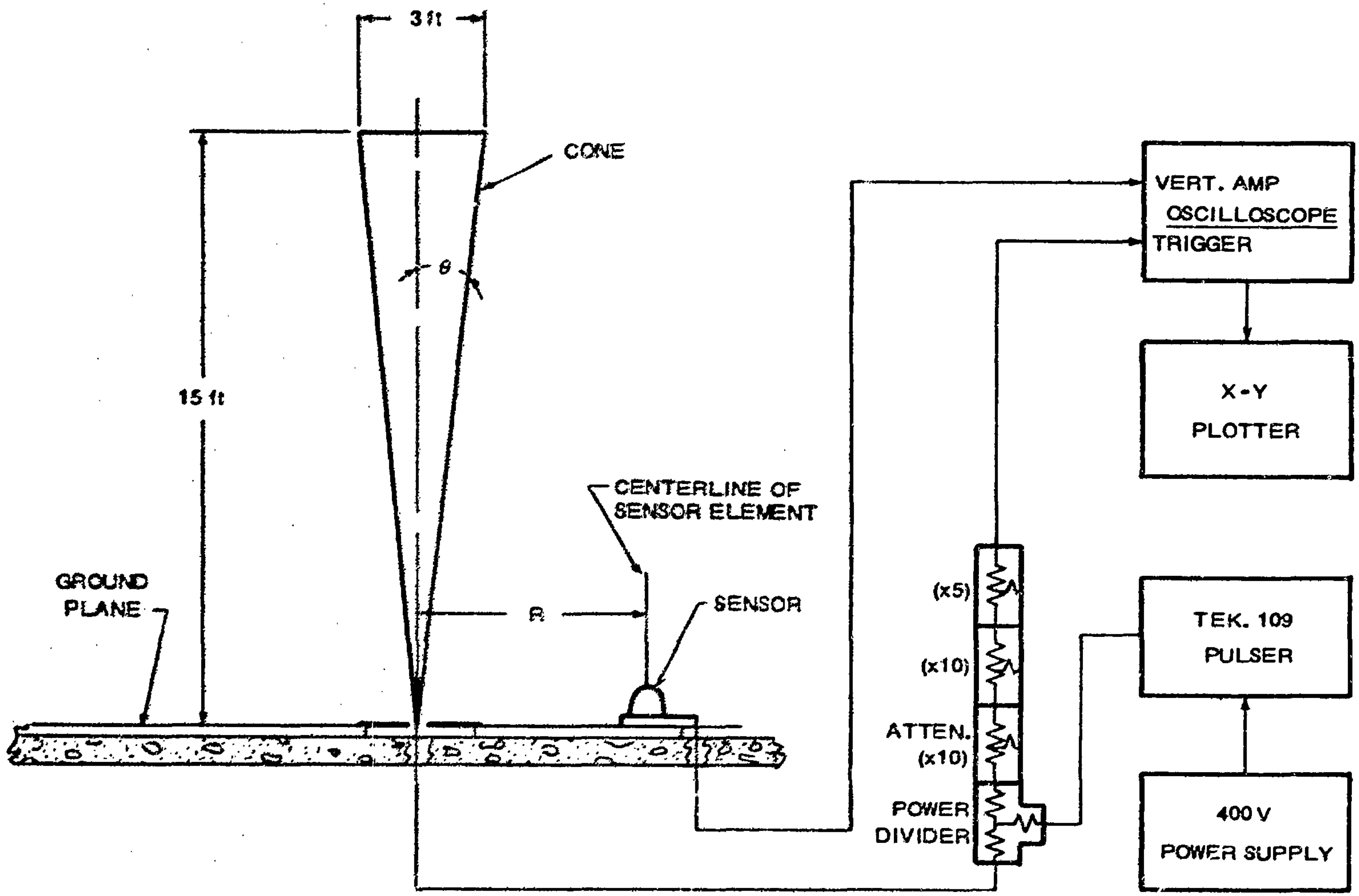

Figure 8. Test Setup for Large Prototype ACD-S1A

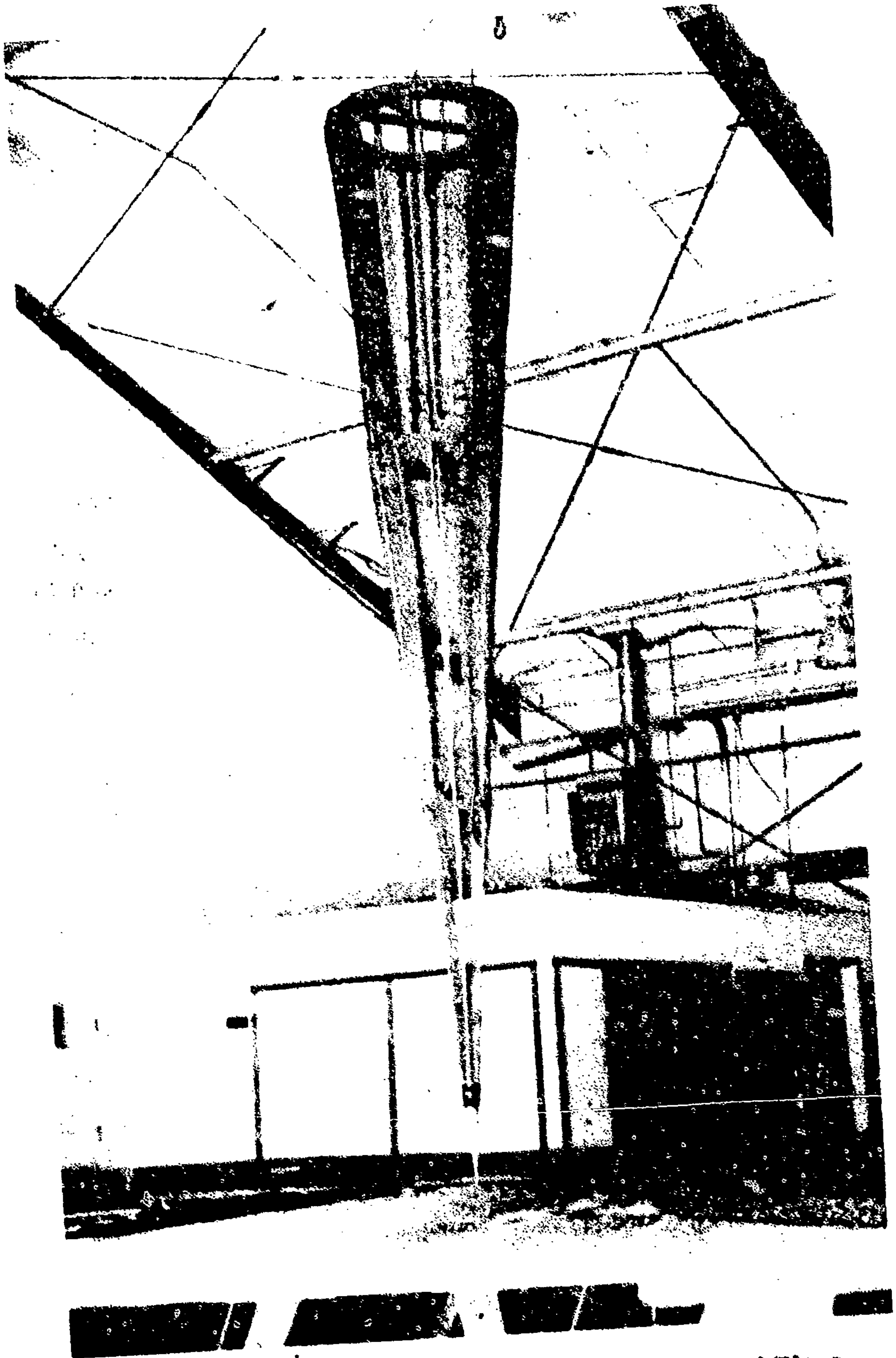

Figure 9. Conical Test Fixture on Elevated Ground Plane

- A Tektronix 109 pulser, with a Spiro-flex charge line is charged to 400 Vdc and used to drive the conical fixture through one side of a power divider and another length of Spiro-flex cable. The other half of the divided signal is used (with various attenuators) to trigger the oscilloscope. The pulser and recording system are shown in Figure 10.
- The sensor output is brought to the sampling oscilloscope, via Spiro-flex cable, and plotted.

b. Risetime

The risetime was measured from the output waveforms taken as indicated above. A 1/4 inch high probe on the ground plane was used to measure the measurement system risetime. The small size of the probe insures a frequency response much greater than that of the rest of the system. It was found, using the "width at half-max" definition of risetime, to be 0.21 ns (Figures 11 and 12). The sensor risetime can be calculated from the sensor and system output and the system risetime using

$$T_r \text{ sensor} = \sqrt{(T_{r \text{ output}})^2 - (T_{r \text{ system}})^2} \qquad (14)$$

From Figure 13, the recorded response from the sensor, $T_{r \text{ output}}$ is found to be about 0.45 ns. Substituting into the above equation, the sensor risetime is about 0.40 ns. This implies a frequency response of 880 MHz for the ACD large prototype, assuming the standard relation of T_r BW=0.35. Scaling this down to the actual ACD-1A size implies a bandwidth of 8.8 GHz. At this time it must be pointed out that horizontal scale calibration data using a laboratory standard was not taken although the scope was within its calibration period. It should also be noted that a sampling system can be incorrectly adjusted, during "calibration" to give an apparent risetime faster than that actually present.

c. Sensitivity

The sensitivity measurements were comparative. The output of the ACD-1 large prototype was recorded and then a HSD-3B(R) sensor was placed in the same location and the measurement repeated. Referring to Figure 13, the area under the ACD large prototype output waveform is calculated as follows:

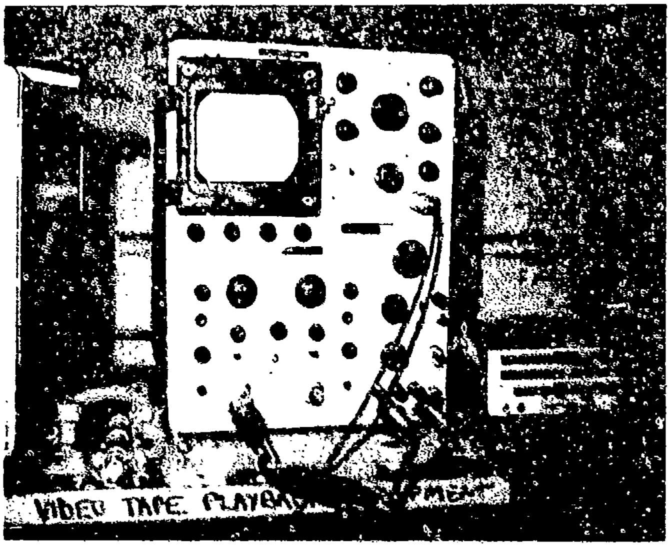

a. Tektronix 661 Scope with 452A Plug In (T_r = 90 psec)

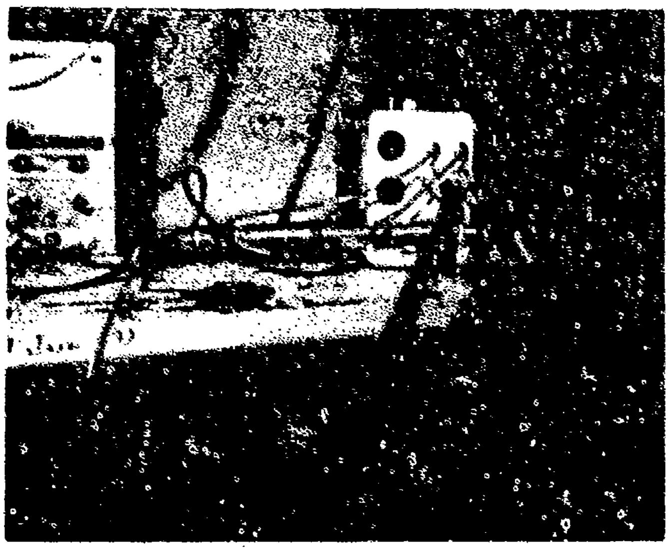

b. Tektronix 109 Pulser with Spiroflex Cables

Figure 10. Pulser and Recording Equipment

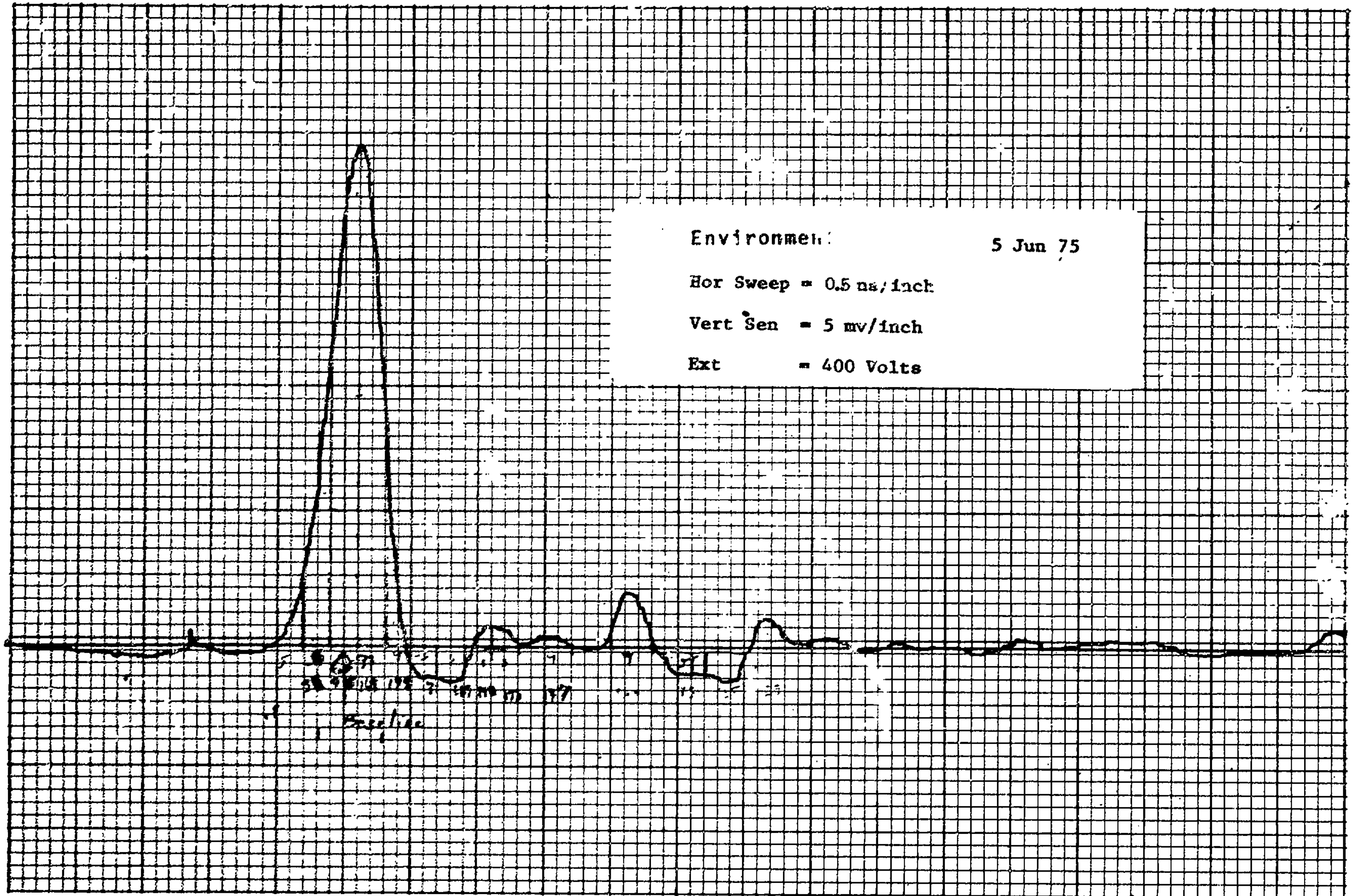

Figure 11. Response of 1/4 inch High Test Probe

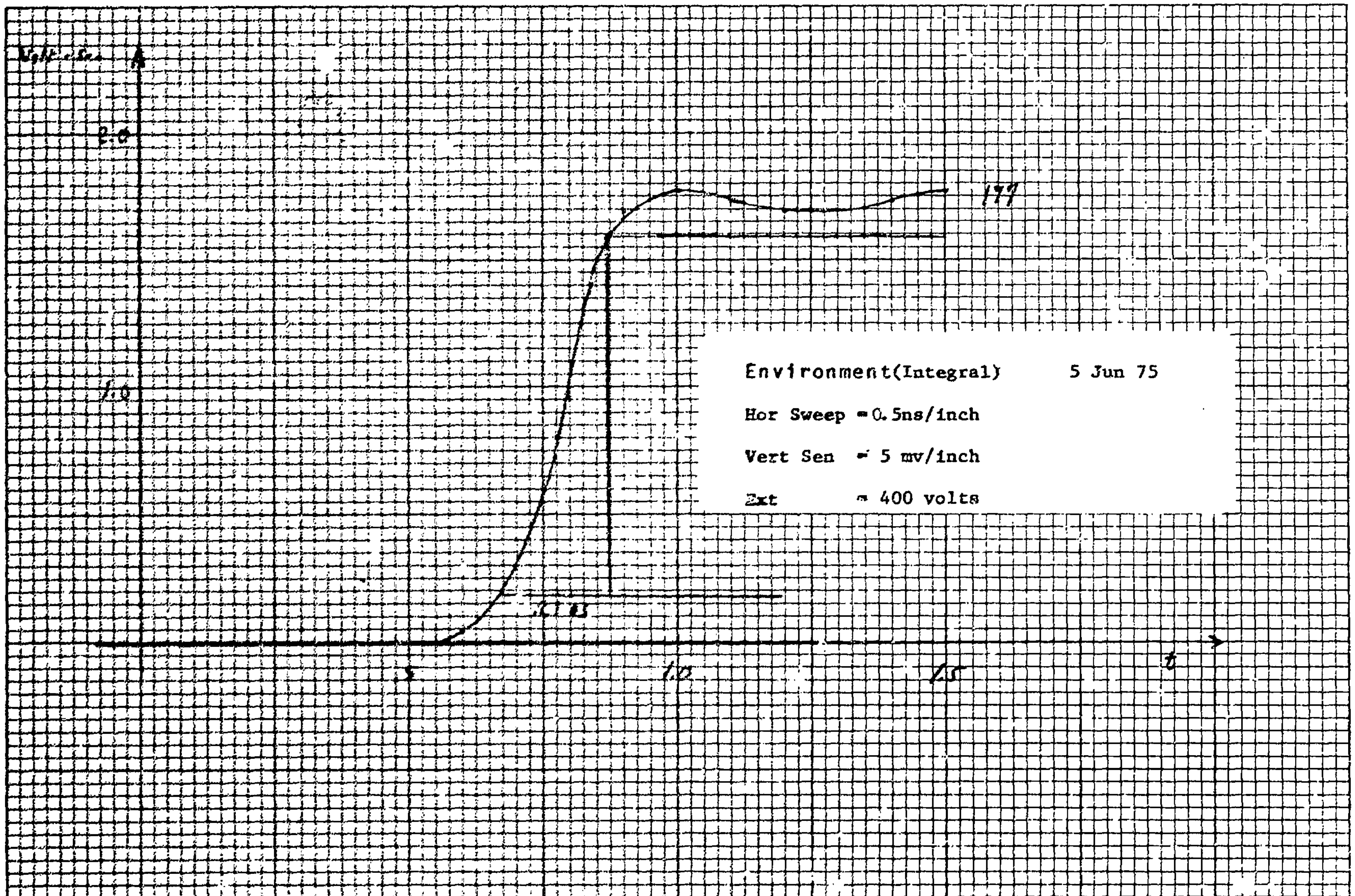

Figure 12. Integrated Response of 1/4 inch High Test Probe

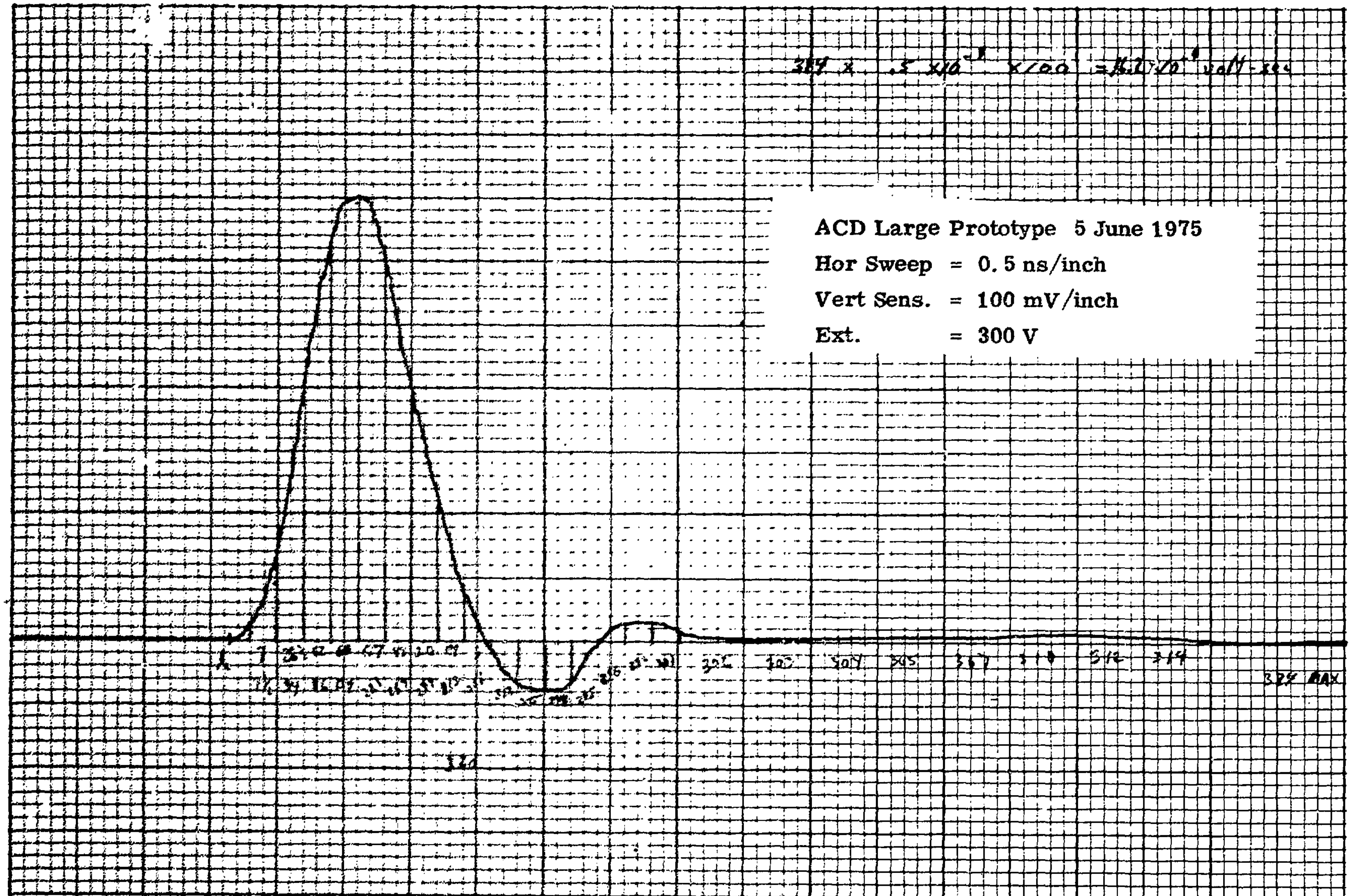

Figure 13. Output of ACD Large Prototype

$$\int_{ACD} V_o\,dt = 324 \text{ squares} \times 0.5 \times 10^{-4} \text{ sec/in} \times 0.1 \text{ V/in} \times \frac{\text{in}^2}{100 \text{ square}} \times (1.11)$$

$$= 0.180 \text{ V-sec}$$

The total correction factor (1.11) was obtained from Figure 14 which is a calibration plot for the vertical sensitivity. The 100 mV data are to be corrected by 1.11 and the 50 mV data are to be corrected by 1.042.

Similarly, using the latter correction factor and the information in the HSD-3B(R) output data in Figure 15, the following is obtained

$$\int_{HSD} V_o\,dt = 328 \text{ squares } 1 \times 10^{-4} \text{ sec/in} \times 0.05 \text{ V/in} \times \frac{\text{in}^2}{100 \text{ square}} \times (1.042)$$

$$= 0.1709 \text{ V-sec}$$

This implies that the ACD large prototype is 5.33% larger than the HSD-3B(R). Recall that this is in addition to the 2% correction applied at the time of initial design.

One of the scaling inaccuracies of this model is in the output connector. The GR 874 is small in relation to the prototype ACD, but the OSSM 274 is much larger than the actual ACD sensing element. At a later date, a test was performed in the setup of Figure 8. This was an effort to get an indication of the effect large connector block has on the sensor pulse response. A 2 inch by 5 inch by 6 inch piece of styrofoam was covered with aluminum foil and placed over the GR connector. The sensor output was recorded, the styrofoam block removed and the output was recorded again. Figure 17 shows the reflection from the connector at about four nanoseconds. That is the round trip time between the connector and the sensing element. The Sensor was positioned so the connector was farthest from the incident wave and in line with the sensing element and cone apex.

d. **TDR Response**

The TDR signature in Figure 16 was obtained through the output connector. The characteristic impedance of 50 ohms is preserved throughout the wiring up to the eventual open circuit at the sensing element, allowing for minor discontinuties at the connections.

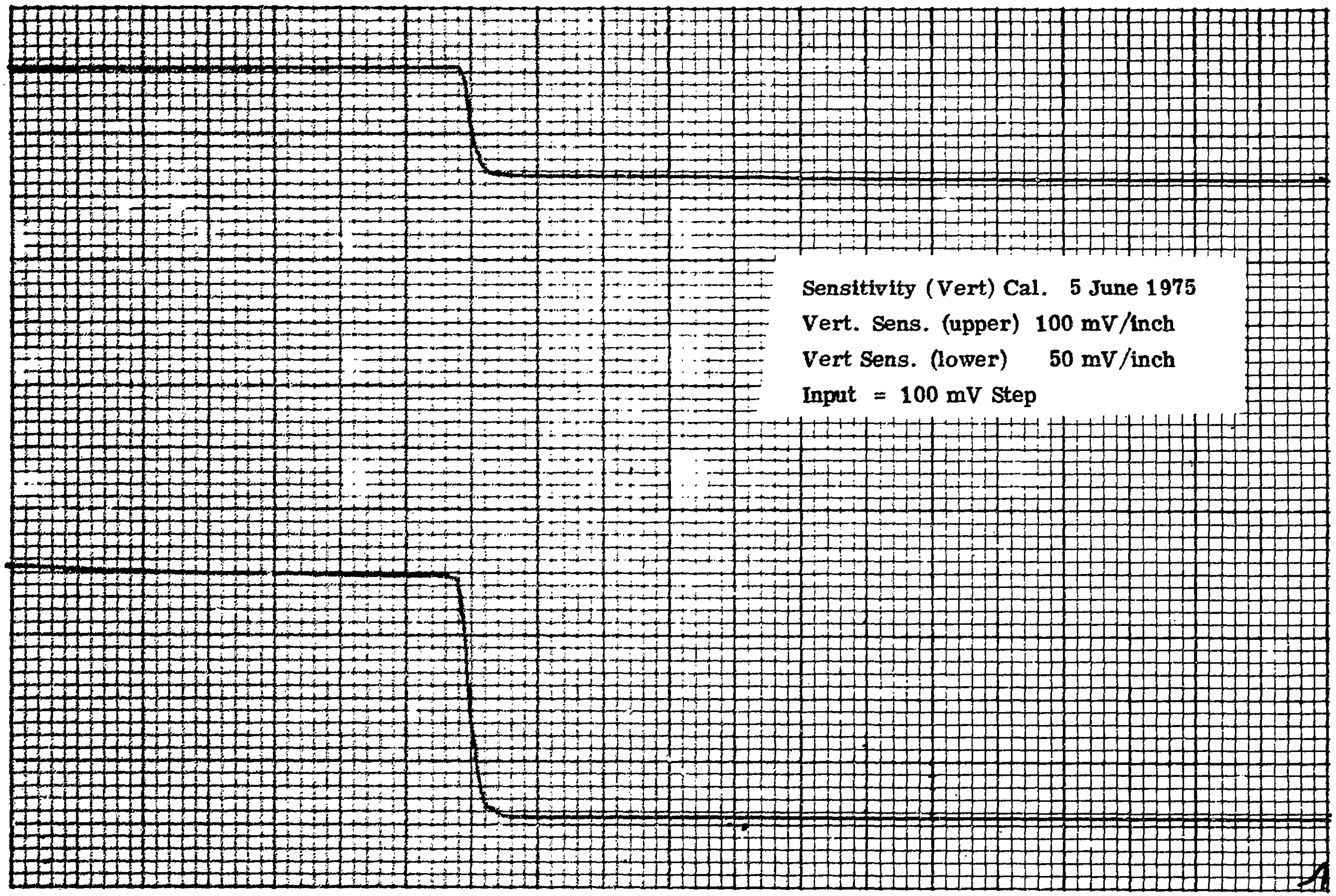

Figure 14. Vertical Amplitude Calibration Plot

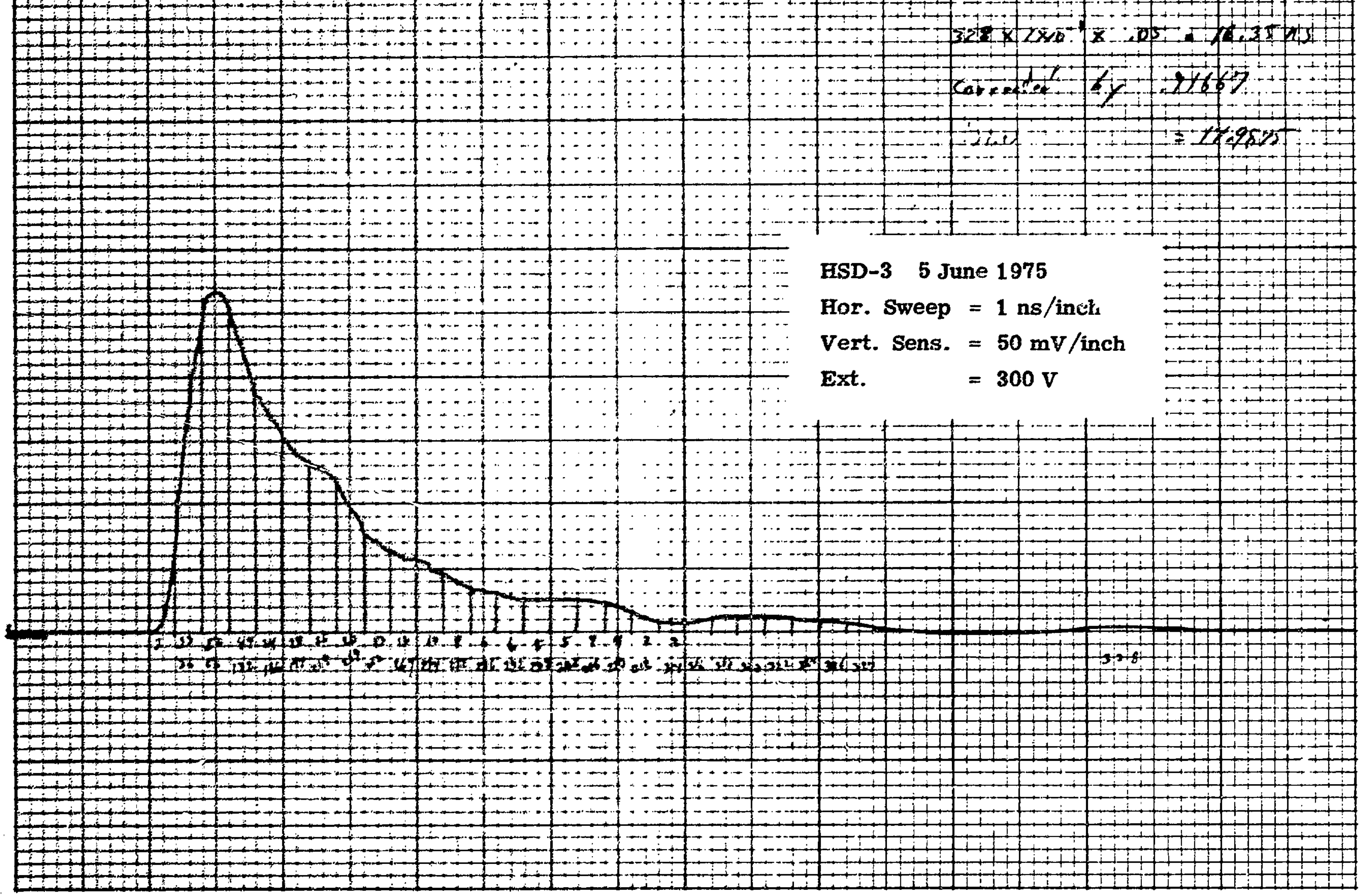

Figure 15. Output of HSD-3

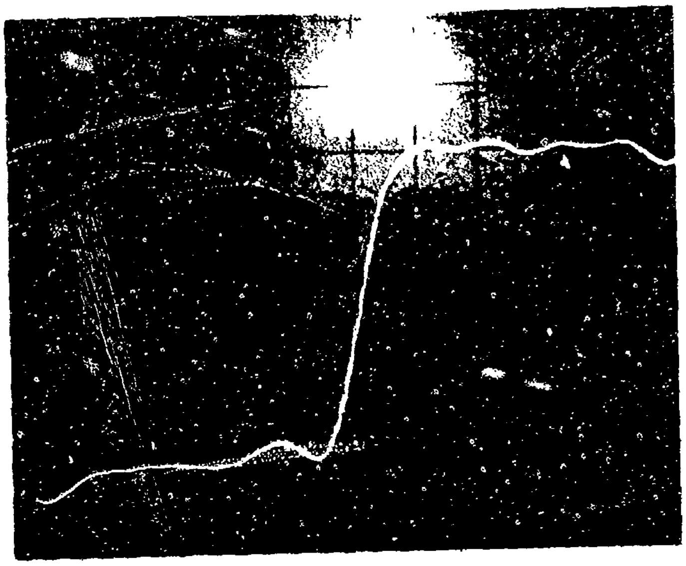

Figure 16. TDR Response of ACD-1 Large Prototype

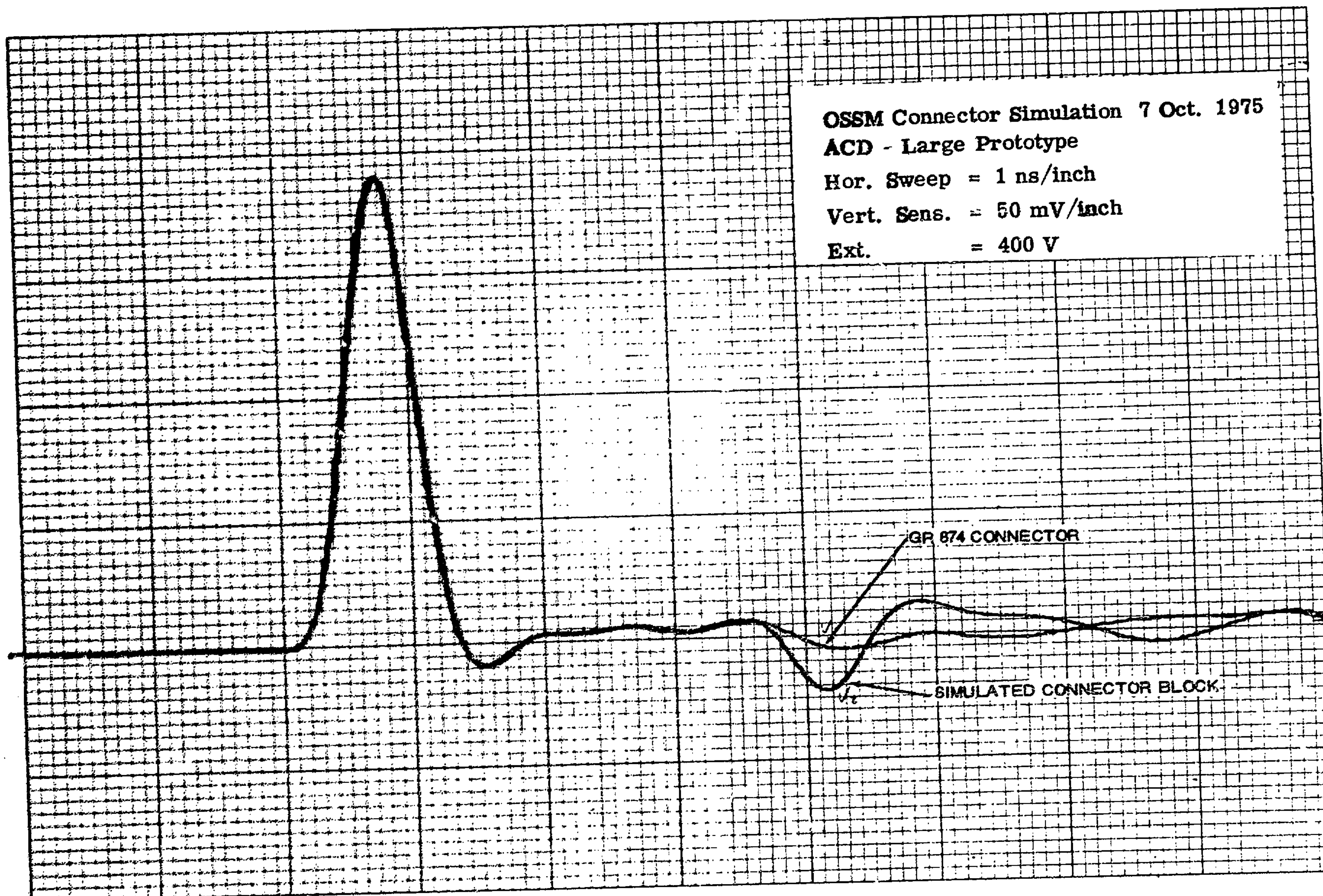

Figure 17. Simulation of an OSSM 274 Connector on the ACD Large Prototype

SECTION IV

ACD-S1A(R) D-DOT SENSOR

The design and construction of the actual ACD is identical to that of the large prototype model. The material sizes and dimensions used on the prototype were scaled up based on what was available in the size appropriate for the ACD-S1A. Rather than proceed to recalculate the scaled dimensions and specifications, only the modified or otherwise different features will be covered.

1. DIMENSION CALCULATIONS AND SENSITIVITY

Based on the large prototype tests (Section III, paragraph 5.), the equivalent area was reduced by a total of 9.5% from calculated values to compensate for perturbations due to the ground plane, dome, etc. This is to ensure that the equivalent area of the ACD-1 is one tenth that of an HSD-3. The calculations are performed in Appendix A.

It should be noted that the data of Section III, paragraph 5. indicate 5.3% or a total of 7.3% for the applied reduction. The 9.5% reduction was based on data that were found to be in error. At the time of this writing, further investigation is underway.

The dimensions of the baseplate were chosen to be 0.40 inch thick x 1.0 inch diameter, .374 inch wide stem protruding from one edge run to the connector, see Figure 1. The sensor has a mass of 12 g (0.4 oz.).

The base plate of the ACD-S1B(R) version is the same with the exception of a 1-1/4 inch length of 0.005 inch thick brass replacing a portion of the stem between the sensing element and connector. The 50Ω output cable is on top of the flexible ground plane and bonded to it. This permits some conforming to cylindrical surfaces--but semi-rigid coaxial cable is not designed to be bent frequently.

2. FREQUENCY LIMITATIONS

The 7.5% reduction of equivalent area over the prototype will cause a corresponding risetime change due to the lowering of the sensor capacitance and decreased transit times. From Appendix A, C is 0.163 pF and the resulting RC risetime is $T_r = 18$ psec. The transit time limitation, as discussed in Section III, paragraph 4., will also become about 7.5% smaller than the

scaled ACD-prototype risetime-about 41 psec. Adding the transit limitation and inductive limitation in quadrature gives

$$T_r = 45 \text{ psec}$$

for the risetime of the ACD-S1A and implies a bandwidth of 7.8 GHz.

3. HIGH VOLTAGE DESIGN

The maximum voltage output will be limited by the Teflon washer at the base of the sensing element. Using a surface flashover strength of 10 kV/inch and a washer with an inside radius of 0.005 inch and outside radius of 0.0175 inch, 125 V is the calculated maximum voltage to be applied between the sensing element and the ground plate. This corresponds to an incident pulse with an electric field component of over 2 MV/meter rising in 1 ns.

4. PULSE RESPONSE

Based on the test results of the large prototype, the ACD-S1A(R) should exhibit a frequency response (upper 3 dB point) in excess of 7.5 GHz.

5. TDR RESPONSE

Figure 18 shows the TDR of a typical ACD-S1A(R) sensor. Slight impedance deviations are present at the connector. Since the sensor is extremely small, the contribution of the sensing element is not readily discernable from the open circuit which immediately follows.

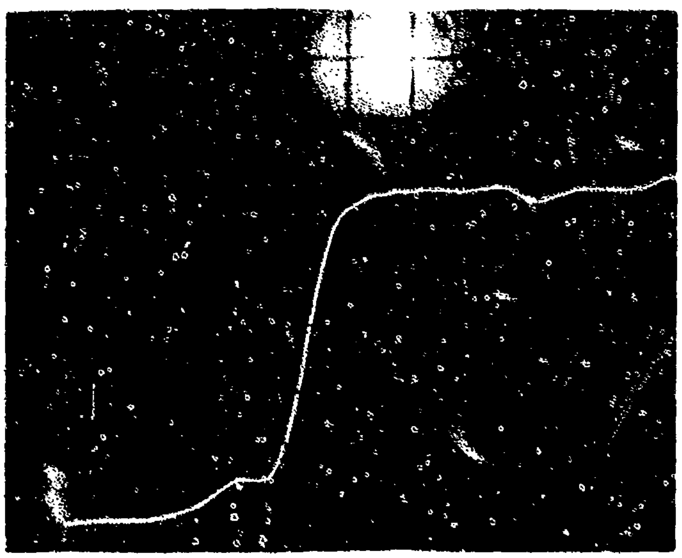

Figure 18. TDR Response of ACD-1 Large Prototype

SECTION V
CONCLUSIONS

The ACD-S1A(R) D-dot sensor may now be considered to be operational and available for determination of electric field changes. Its frequency response is approximately 7.5 GHz.

The small physical size of the sensor and the air environment surrounding the sensing element result in a maximum safe output of about 125 V. This specification implies a high incident field (2 MV/meter) associated with the incident TEM wave.

The output connector should be reduced in size to minimize the field perturbation and subsequent reflections which effect the sensor output (See Figure 18). This would also reduce the probability of flashover in very intense E-field environments.

APPENDIX A
EQUIVALENT AREA DETERMINATION

The shape of the ACD-S1A(R) D-dot sensor is determined from equations derived by C. E. Baum.[2] These describe a technique for obtaining the potential distribution of a line charge of known height and charge density. The sensor surface is then chosen as one of these equipotential surfaces. The capacitance and dipole moment can then be found by integration, yielding the low frequency parameters. A conical transmission line at the apex provides the high frequency limitation of SSN 69.[5]

A.1 GEOMETRY

First the impedance of the conical center portion is selected as 50 ohms – this is the desired load impedance from SSN 36.[4] The impedance is given by.

$$Z_c = \frac{1}{2\pi}\sqrt{\frac{\mu_o}{\epsilon_o}}\ln\left(\cot\frac{\theta_o}{2}\right) \tag{A-1}$$

where θ_o is the angle of the cone with respect to a vertical line passing through its axis as illustrated in Figure A-1. For Z_o of 50 ohm, we can define

$$\Phi_o \equiv \mathrm{Tan}\left(\frac{\theta_o}{2}\right) = \exp\frac{-Z_o 2\pi}{\sqrt{\mu_o/\epsilon_o}} = 0.4343476 \tag{A-2}$$

Also from SSN 72 we have

$$\frac{h_{eff}}{h_{geo}} = \sqrt{1-\Phi_o^{\,2}} \tag{A-3}$$

and

$$C = -\epsilon_o\, h_{eff}\, \pi\, \frac{\sqrt{1-\Phi_o^{\,2}}}{\ln\Phi_o} \tag{A-4}$$

[5] Baum, Carl E., Design of a Pulse-Radiating Dipole Antenna as Related to High-Frequency and Low-Frequency Limits, 13 Jan. 69, AFWL SSN 69.

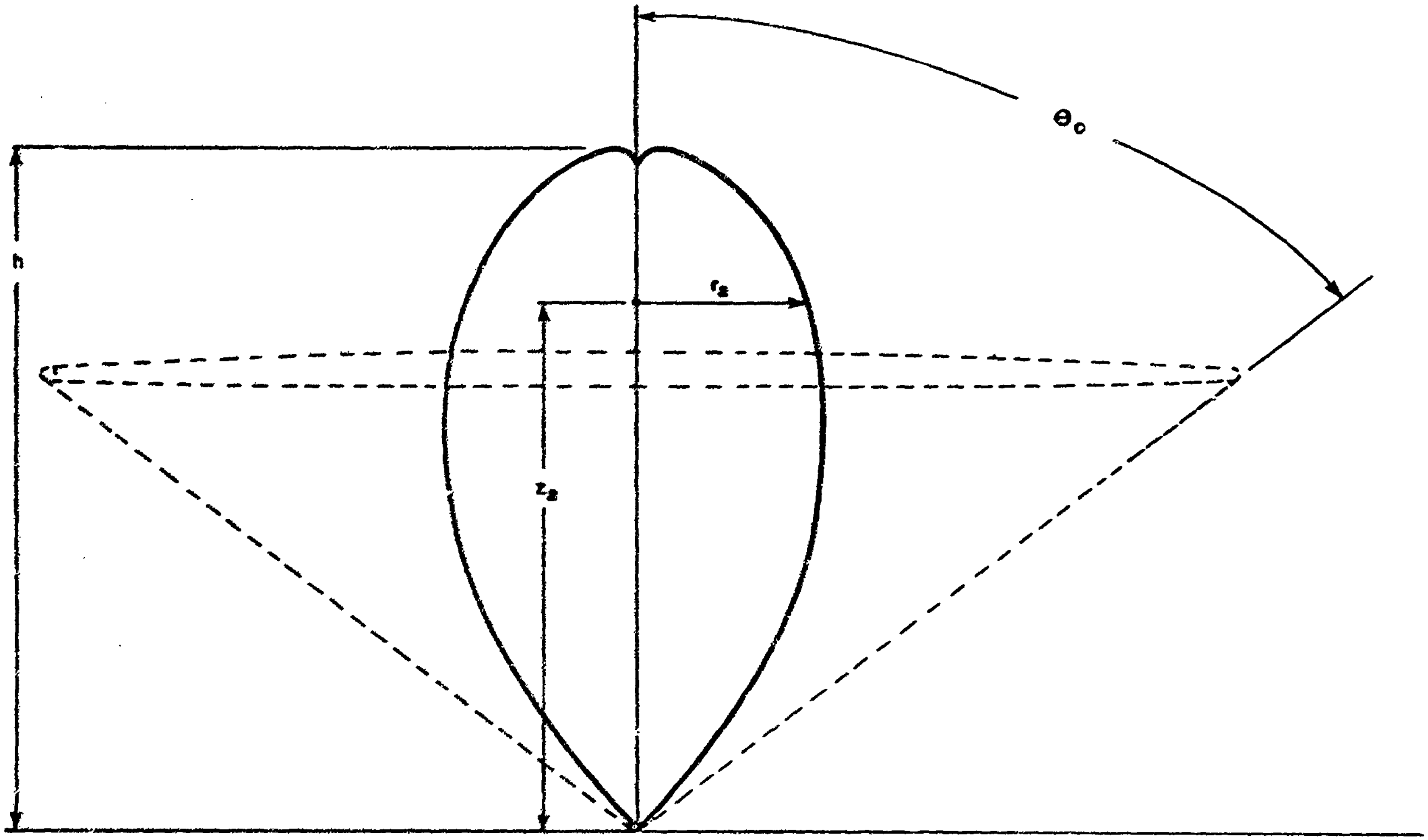

Figure A-1 ACD Geometric Parameters

where

h_{eff}	=	height of equivalent charge
h_{geo}	=	actual height of sensor
C	=	capacitance of sensor with respect to image surface
ϵ_o	=	dielectric constant of material around sensor (assumed, for calculations, to be free space)

The area can be defined in terms of the capacitance and the equivalent height, h_{eff} as

$$A_{eq} = h_{eff} \frac{C}{\epsilon_o}$$

which implies that

$$h_{geo} = \sqrt{\frac{A_{eq}}{\pi} \left(\frac{-\ln \Phi_o}{1 - \Phi_o^2} \right)}$$

Now that all the physical parameters have been defined, SSN 72[2] gives the conditions necessary to obtain values of z and r in a cylindrical coordinate system, such that the surface evolved by rotation is on an equipotential surface of the original assumed line charge.

$$\frac{1}{\Phi_o} = \left[\frac{z}{r} + \sqrt{\frac{z^2}{r^2} + 1} \right] x \sqrt{\frac{(h_{geo} - z) + \sqrt{(h_{geo} - z)^2 + r^2}}{(h_{geo} + z) + \sqrt{(h_{geo} + z)^2 + r^2}}} \qquad \text{(A-5)}$$

This equation can now simply be iterated at various values of z to find the corresponding r that defines a data point (z, r) on the equipotential surface. This can be done for z ranging from zero to h_{geo} at which point r = 0 defines the top of the asymtotic conical dipole.

The following pages describe the program and results for the large prototype and the production for ACD-S1A sensors.

A-2. PROGRAM AND RESULTS

The following is the computer program used to generate the asymtotic conical dipole sensor (ACD-S1A(R)) and its large prototype. Where:

110	E0	=	ϵ_o, permitivity of medium surrounding sensor
120	ZF	=	$\frac{377}{2\pi}\sqrt{\frac{\mu_r}{\epsilon_r}}$, impedance of medium surrounding sensor ($\mu_r \approx \epsilon_r \approx 1$ for air)
130	ZC	=	desired pulse impedance of sensor
140	AEQ	=	desired equivalent area of sensor

are the parameters necessarily specified for a particular sensor. The ACD program is reproduced in Figure A-2.

A-3. STEM

The only remaining task is to define a stem that supports the sensing element and provides the connection to the output cable at the base of the dipole. A stem of 0.010 inch was selected for the production model as having adequate strength and minimum thickness (0.1 inch diameter for the large prototype). After the computer program generated a set of data points, an arc was inscribed which is tangent to the 0.005 inch radius of the stem at the ground plane and also tangent to the data point surface (see Figure A-3). This provides a smooth transition from the cylindrical coaxial line to the conical dipole sensing element. Figure A-3 shows the graphic determination of the transition coordinates. These are manually inserted into the data printout to provide a complete data set for machining the sensing element. Figure A-6 shows the shifted coordinate system used in the data output.

```
LIST

ACD         08:51MDT    07/10/75

REAL LNT,Z(3000),R(3000)
E0=8.8542E-12
ZF=59.9584916
ZC=50.0
AEQ=1.0E-4
LNT=ZC/ZF
TINV=EXP(LNT)
THETA=1.0/TINV
PI=3.1415926536
RAD=SQRT(1.0-THETA*THETA)
CORR=0.905
AE=AEQ*CORR
H=SQRT(AE*LNT/PI)/RAD
CAP=E0*PI*H*RAD/LNT
H=H*39.37
INC=1000
STEP=1.0/INC
IH=H*INC+2
BETA=0.35/(2.2*50.0*CAP)
I=1
TAU=0.35/BETA
Z0=H*RAD
Z(1)=0.0
R(1)=0.0
Q=0.0001

   100 I=I+1
   RN=0.0
   RP=1.0
   A=0.5
   IF(I.GE.IH) GOTO 900
   Z(I)=(I-1)*STEP
   X=H-Z(I)

       200 CONTINUE
       C=Z0+X
       D=Z0-X
       E=(D+SQRT(D*D+A*A))/(C+SQRT(C*C+A*A))
       THTINV=(X/A+SQRT((X*X/A/A)+1))*SQRT(E)
       T=THTINV-TINV
       IF(Q-ABS(T))300,600,600

          300 IF(T)400,500,500

             400 RP=A
             A=(A+RN)/2.
             GO TO 200

             500 RN=A
             A=(A+RP)/2.
             GO TO 200

   600 R(I)=A
   IF(A.GT.R(I-1)) RMAX=A
   GO TO 100

900 CONTINUE
PRINT,"     EQUIVALENT AREA:",AEQ,"  SQUARE METERS"
PRINT,"     CORRECTION FACT:",CORR
PRINT,"     THETA INVERSE:   ",TINV
PRINT,"     SENSOR HEIGHT:   ",H," INCHES"
PRINT,"     CAPACITANCE:     ",CAP," FARADS"
PRINT,"     BANDWIDTH:       ",BETA," HERTZ"
PRINT,"     10/90 RISETIME   ",TAU," SECONDS"

   DO 520 I=1,IH
   520 R(I)=RMAX-R(I)

MM=1
MR=(IH/40+1)*10
PRINT," "
PRINT,"     THIS TABLE GIVES Z,R  DATA PAIRS - IN INCHES"
PRINT," "

   DO 530 I=1,MR,MM
   I2=I+MR
   I3=I2+MR
   I4=I3+MR
   PRINT 537,Z(I),R(I),Z(I2),R(I2),Z(I3),R(I3),Z(I4),R(I4)
   537 FORMAT(1X,4(4X,F5.3,2X,F6.4))
   530 CONTINUE

999 STOP; END
```

Figure A-2. Program for Computing the ACD Shape

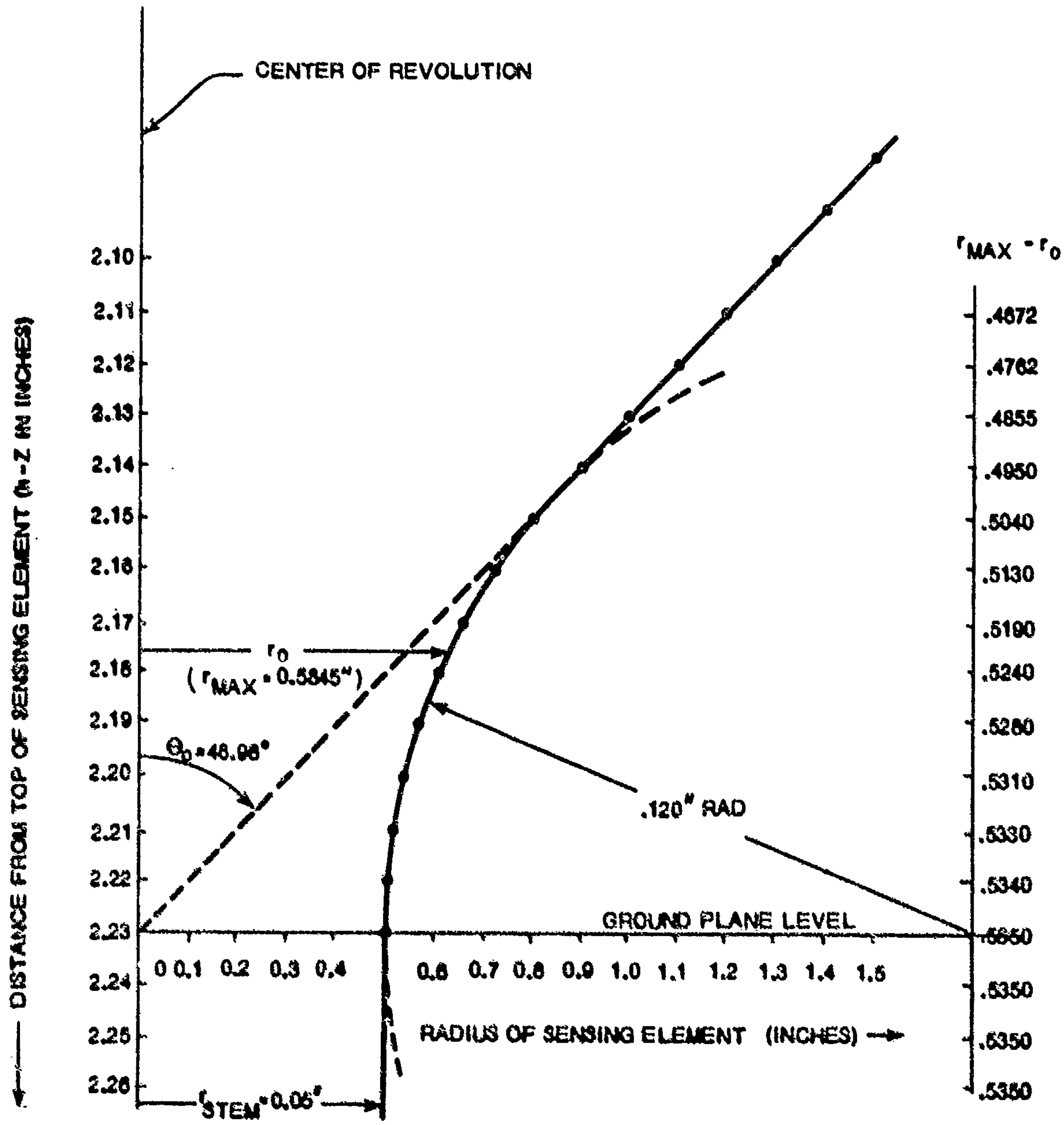

Figure A-3. Stem Dimensions and Radius Calculations for ACD Prototype

A-4. RESULTS

Figure A-4 lists the data pairs (z, r) for the generation of the ACD large prototype sensor with an equivalent area of $10^{-2} m^2$. The first coordinate of the pair z, r, describes the height above the ground plane. The coordinate origin has been shifted to the z_{max} and r_{max} of the sensor for ease of machining so that $z = h$ implies ground plane level (see Figure A-6). The stem, of course, will be longer and z continues as the stem penetrates the ground plane.

The second page following has similar data for the actual ACD-S1A(R) D-dot sensor (Figure A-5).

EQUIVALENT AREA: 1.0000000E-02 SQUARE METERS
CORRECTION FACT: 9.8000000E-01
THETA INVERSE: 2.3023037E+00
SENSOR HEIGHT: 2.2292621E+00 INCHES
CAPACITANCE: 1.7012873E-12 FARADS
BANDWIDTH: 1.8702416E+09 HERTZ
10/90 RISETIME 1.8714160E-10 SECONDS

THIS TABLE GIVES Z,R DATA PAIRS - IN INCHES.

0.	0.5845	0.600	0.0342	1.200	0.0235	1.800	0.2411
0.010	0.4970	0.610	0.0321	1.210	0.0257	1.810	0.2471
0.020	0.4613	0.620	0.0301	1.220	0.0273	1.820	0.2530
0.030	0.4337	0.630	0.0281	1.230	0.0290	1.830	0.2588
0.040	0.4114	0.640	0.0262	1.240	0.0311	1.840	0.2649
0.050	0.3908	0.650	0.0242	1.250	0.0328	1.850	0.2711
0.060	0.3731	0.660	0.0222	1.260	0.0349	1.860	0.2775
0.070	0.3575	0.670	0.0202	1.270	0.0371	1.870	0.2838
0.080	0.3420	0.680	0.0187	1.280	0.0392	1.880	0.2902
0.090	0.3287	0.690	0.0170	1.290	0.0413	1.890	0.2968
0.100	0.3156	0.700	0.0156	1.300	0.0434	1.900	0.3035
0.110	0.3036	0.710	0.0139	1.310	0.0461	1.910	0.3100
0.120	0.2915	0.720	0.0131	1.320	0.0482	1.920	0.3170
0.130	0.2808	0.730	0.0117	1.330	0.0508	1.930	0.3240
0.140	0.2704	0.740	0.0104	1.340	0.0534	1.940	0.3310
0.150	0.2601	0.750	0.0093	1.350	0.0560	1.950	0.3381
0.160	0.2503	0.760	0.0082	1.360	0.0586	1.960	0.3453
0.170	0.2411	0.770	0.0072	1.370	0.0611	1.970	0.3528
0.180	0.2326	0.780	0.0061	1.380	0.0642	1.980	0.3602
0.190	0.2240	0.790	0.0051	1.390	0.0667	1.990	0.3677
0.200	0.2160	0.800	0.0046	1.400	0.0698	2.000	0.3753
0.210	0.2094	0.810	0.0039	1.410	0.0728	2.010	0.3832
0.220	0.2004	0.820	0.0029	1.420	0.0758	2.020	0.3910
0.230	0.1930	0.830	0.0025	1.430	0.0788	2.030	0.3990
0.240	0.1863	0.840	0.0021	1.440	0.0817	2.040	0.4071
0.250	0.1791	0.850	0.0014	1.450	0.0851	2.050	0.4153
0.260	0.1724	0.860	0.0011	1.460	0.0886	2.060	0.4237
0.270	0.1662	0.870	0.0003	1.470	0.0919	2.070	0.4322
0.280	0.1597	0.880	0.0003	1.480	0.0953	2.080	0.4406
0.290	0.1539	0.890	0.0003	1.490	0.0986	2.090	0.4495
0.300	0.1483	0.900	0.	1.500	0.1019	2.100	0.4583
0.310	0.1427	0.910	0.	1.510	0.1057	2.110	0.4672
0.320	0.1370	0.920	0.	1.520	0.1095	2.120	0.4762
0.330	0.1316	0.930	0.	1.530	0.1132	2.130	0.4855
0.340	0.1264	0.940	0.	1.540	0.1169	2.140	0.4950
0.350	0.1215	0.950	0.	1.550	0.1210	2.150	0.5040
0.360	0.1167	0.960	0.	1.560	0.1246	2.160	0.5130
0.370	0.1120	0.970	0.0006	1.570	0.1286	2.170	0.5190
0.380	0.1073	0.980	0.0011	1.580	0.1326	2.180	0.5240
0.390	0.1026	0.990	0.0011	1.590	0.1370	2.190	0.5280
0.400	0.0981	1.000	0.0017	1.600	0.1414	2.200	0.5310
0.410	0.0943	1.010	0.0023	1.610	0.1453	2.210	0.5330
0.420	0.0899	1.020	0.0028	1.620	0.1496	2.220	0.5340
0.430	0.0861	1.030	0.0034	1.630	0.1542	2.230	0.5350
0.440	0.0825	1.040	0.0046	1.640	0.1588	2.240	0.5350
0.450	0.0785	1.050	0.0051	1.650	0.1634	2.250	0.5350
0.460	0.0748	1.060	0.0057	1.660	0.1679	2.260	0.5350
0.470	0.0711	1.070	0.0068	1.670	0.1728	2.270	0.5350
0.480	0.0680	1.080	0.0079	1.680	0.1776	2.280	0.5350
0.490	0.0647	1.090	0.0095	1.690	0.1823	2.290	0.5350
0.500	0.0612	1.100	0.0096	1.700	0.1874	2.300	0.5350
0.510	0.0582	1.110	0.0108	1.710	0.1925	2.310	0.535
0.520	0.0553	1.120	0.0119	1.720	0.1974	2.320	0.5350
0.530	0.0519	1.130	0.0135	1.730	0.2027	2.330	0.5350
0.540	0.0494	1.140	0.0147	1.740	0.2079	2.340	0.5350
0.550	0.0468	1.150	0.0158	1.750	0.2130	2.350	0.5350
0.560	0.0440	1.160	0.0174	1.760	0.2198	2.360	0.5350
0.570	0.0415	1.170	0.0191	1.770	0.2241	2.370	0.5350
0.580	0.0388	1.180	0.0202	1.780	0.2298	2.380	0.5350
0.590	0.0365	1.190	0.0219	1.790	0.2353	2.390	0.5350

Obtained manually from Figure A-3

Figure A-4. Coordinates for ACD Large Prototype

EQUIVALENT AREA: 1.0000000E-04 SQUARE METERS
CORRECTION FACT: 9.0500000E-01
THETA INVERSE: 2.3023037E+00
SENSOR HEIGHT: 2.1422610E-01 INCHES
CAPACITANCE: 1.6348914E-13 FARADS
BANDWIDTH: 1.9461955E+10 HERTZ
10/90 RISETIME 1.7983805E-11 SECONDS

THIS TABLE GIVES Z,R DATA PAIRS - IN INCHES

0.	0.0562	0.060	0.0028	0.120	0.0032	0.180	0.0275
0.001	0.0476	0.061	0.0026	0.121	0.0034	0.181	0.0281
0.002	0.0441	0.062	0.0024	0.122	0.0036	0.182	0.0288
0.003	0.0414	0.063	0.0022	0.123	0.0038	0.183	0.0295
0.004	0.0392	0.064	0.0020	0.124	0.0040	0.184	0.0301
0.005	0.0373	0.065	0.0019	0.125	0.0042	0.185	0.0308
0.006	0.0355	0.066	0.0017	0.126	0.0045	0.186	0.0315
0.007	0.0339	0.067	0.0016	0.127	0.0047	0.187	0.0322
0.008	0.0325	0.068	0.0014	0.128	0.0050	0.188	0.0330
0.009	0.0311	0.069	0.0013	0.129	0.0052	0.189	0.0337
0.010	0.0298	0.070	0.0011	0.130	0.0055	0.190	0.0344
0.011	0.0286	0.071	0.0010	0.131	0.0057	0.191	0.0352
0.012	0.0275	0.072	0.0009	0.132	0.0060	0.192	0.0359
0.013	0.0264	0.073	0.0008	0.133	0.0063	0.193	0.0367
0.014	0.0254	0.074	0.0007	0.134	0.0066	0.194	0.0375
0.015	0.0245	0.075	0.0006	0.135	0.0069	0.195	0.0383
0.016	0.0235	0.076	0.0005	0.136	0.0072	0.196	0.0391
0.017	0.0226	0.077	0.0004	0.137	0.0075	0.197	0.0399
0.018	0.0218	0.078	0.0004	0.138	0.0078	0.198	0.0408
0.019	0.0210	0.079	0.0003	0.139	0.0081	0.199	0.0416
0.020	0.0202	0.080	0.0002	0.140	0.0084	0.200	0.0425
0.021	0.0194	0.081	0.0002	0.141	0.0087	0.201	0.0433
0.022	0.0187	0.082	0.0001	0.142	0.0091	0.202	0.0442
0.023	0.0179	0.083	0.0001	0.143	0.0094	0.203	0.0451
0.024	0.0173	0.084	0.0001	0.144	0.0098	0.204	0.0460
0.025	0.0166	0.085	0.0000	0.145	0.0101	0.205	0.0470
0.026	0.0160	0.086	0.0000	0.146	0.0105	0.206	0.0479
0.027	0.0153	0.087	0.0000	0.147	0.0109	0.207	0.0488
0.028	0.0147	0.088	0.	0.148	0.0113	0.208	0.0495
0.029	0.0142	0.089	0.	0.149	0.0116	0.209	0.0500
0.030	0.0136	0.090	0.0000	0.150	0.0120	0.210	0.0505
0.031	0.0130	0.091	0.0000	0.151	0.0124	0.211	0.0508
0.032	0.0125	0.092	0.0000	0.152	0.0128	0.212	0.0510
0.033	0.0120	0.093	0.0001	0.153	0.0133	0.213	0.0511
0.034	0.0115	0.094	0.0001	0.154	0.0137	0.214	0.0512
0.035	0.0110	0.095	0.0001	0.155	0.0141	0.215	0.0512
0.036	0.0106	0.096	0.0002	0.156	0.0146	0.216	0.0512
0.037	0.0101	0.097	0.0002	0.157	0.0150	0.217	0.0512
0.038	0.0097	0.098	0.0003	0.158	0.0155	0.218	0.0512
0.039	0.0092	0.099	0.0004	0.159	0.0159	0.219	0.0512
0.040	0.0088	0.100	0.0004	0.160	0.0164	0.220	0.0512
0.041	0.0084	0.101	0.0005	0.161	0.0169	0.221	0.0512
0.042	0.0080	0.102	0.0006	0.162	0.0173	0.222	0.0512
0.043	0.0076	0.103	0.0007	0.163	0.0178	0.223	0.0512
0.044	0.0073	0.104	0.0008	0.164	0.0183	0.224	0.0512
0.045	0.0069	0.105	0.0009	0.165	0.0188	0.225	0.0512
0.046	0.0066	0.106	0.0010	0.166	0.0194	0.226	0.0512
0.047	0.0062	0.107	0.0011	0.167	0.0199	0.227	0.0512
0.048	0.0059	0.108	0.0012	0.168	0.0204	0.228	0.0512
0.049	0.0056	0.109	0.0014	0.169	0.0210	0.229	0.0512
0.050	0.0053	0.110	0.0015	0.170	0.0215	0.230	0.0512
0.051	0.0050	0.111	0.0016	0.171	0.0221	0.	0.
0.052	0.0047	0.112	0.0018	0.172	0.0226	0.	0.
0.053	0.0045	0.113	0.0019	0.173	0.0232	0.	0.
0.054	0.0042	0.114	0.0021	0.174	0.0238	0.	0.
0.055	0.0039	0.115	0.0022	0.175	0.0244	0.	0.
0.056	0.0037	0.116	0.0024	0.176	0.0250	0.	0.
0.057	0.0035	0.117	0.0026	0.177	0.0256	0.	0.
0.058	0.0032	0.118	0.0028	0.178	0.0262	0.	0.
0.059	0.0030	0.119	0.0030	0.179	0.0268	0.	0.

Obtained manually as in Figure A-3.

PROGRAM

Figure A-5. Coordinates for ACD-1A(R) Production D-Dot Sensor

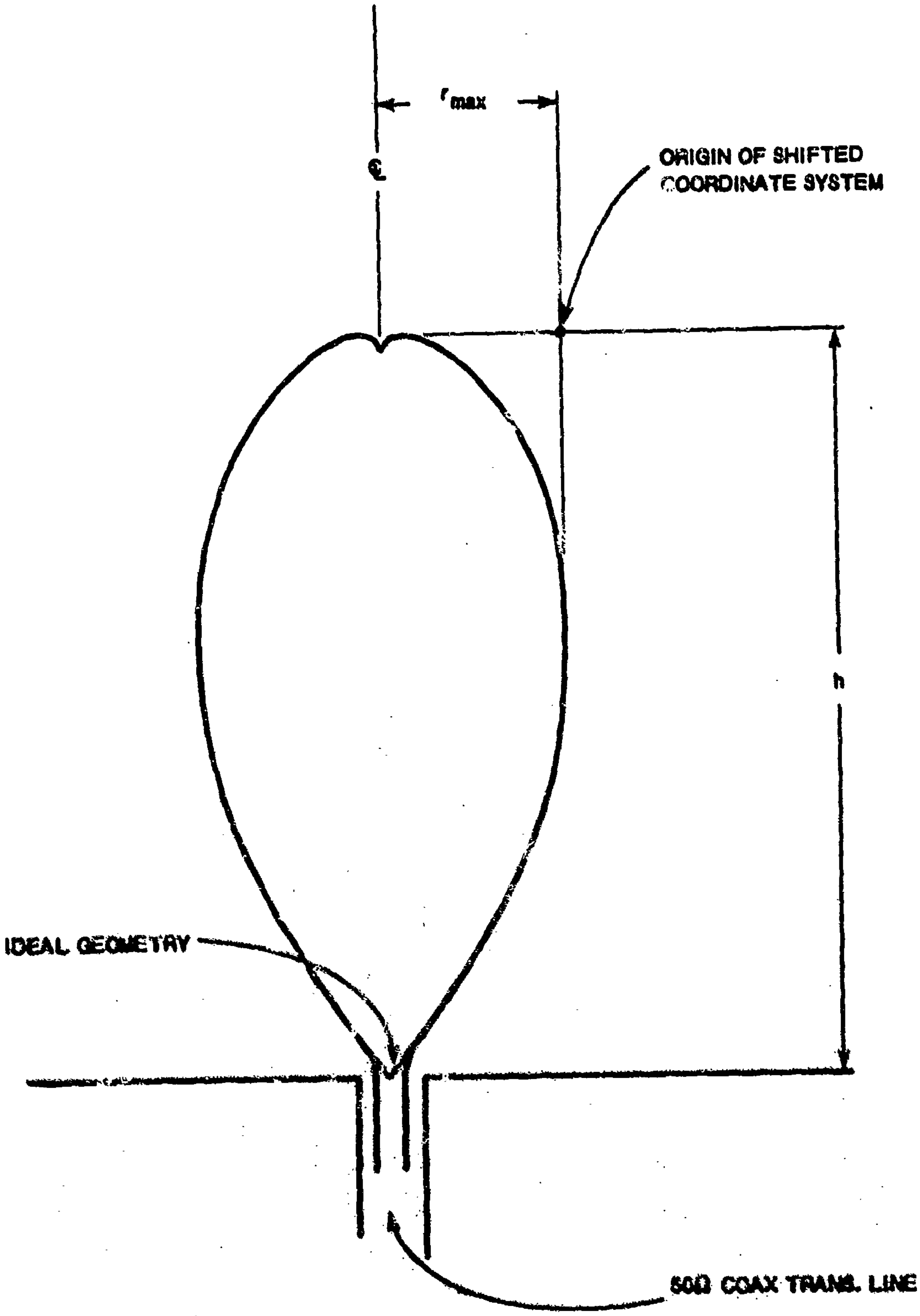

Figure A-6. Coordinate System for ACD Data Coordinates

REFERENCES

1. Olsen, Stewart, MGL-S8(R) B-Dot Sensor Development, 10 September 1975, EG&G Report No. AL-1187, AFWL-TR-75-252.

2. Baum, Carl E., An Equivalent-Charge Method for Defining Geometries of Dipole Antennas, 24 January 1969, AFWL SSN 72.

3. Baum, Carl E., Maximizing Frequency Response of a B-Dot Loop, 9 December 1964, AFWL SSN 8.

4. Baum, Carl E., A Circular Conical Antenna Simulator, 3 March 1967, AFWL SSN 36.

5. Baum, Carl E., Design of a Pulse-Radiating Dipole Antenna as Related to High-Frequency and Low-Frequency Limits, 13 January 1969, AFWL SSN 69.